Carbonate sedimentology and carbon isotope stratigraphy of the Tallbacken-1 core, early Wenlock Slite Group, Gotland, Sweden

Jan Radomski

Dissertations in Geology at Lund University,
Master's thesis, no 526
(45 hp/ECTS credits)

Department of Geology
Lund University
2018

Carbonate sedimentology and carbon isotope stratigraphy of the Tallbacken-1 core, early Wenlock Slite Group, Gotland, Sweden

Master's thesis

Jan Radomski

Department of Geology
Lund University
2018

Contents

Cover Picture: Holmhällars rock field (Sundre formation) Gotland, Sweden.

Carbonate sedimentology and carbon isotope stratigraphy of the Tallbacken-1 core, early Wenlock Slite Group, Sweden

Jan Radomski

Radomski, J., 2018: Carbonate sedimentology and carbon isotope stratigraphy of the Tallbacken-1 core, early Wenlock Slite Group, Gotland, Sweden. Dissertations in Geology at *Lund University*, No.526, 28 pp. 45 hp (45 ECTS credits).

Abstract: The more than 700 m thick carbonate succession of Gotland represents the erosional remnants of a vast carbonate platform system that formed in the Baltic basin during the Silurian Period. This thesis focuses on the stratigraphy and carbonate microfacies of the Tallbacken-1 core that was drilled at Stora Vede by the Swedish Geological Survey in 2006. Carbonate microfacies analysis of the core along with gamma ray log data from the well form basis for interpretation on the depositional environment for the rocks and the evolution of the carbonate platform complex through the corresponding time interval. The five recognized carbonate microfacies associations correspond to five depositional environments. This can be seen in the following ascending order in the core: low energy outer ramp, moderate energy middle ramp, high energy reef slope, high energy reef belt and a relatively low energy lagoonal setting. In addition, 176 whole-rock samples were collected and used for $\delta^{13}C$ analysis to constrain the stratigraphy of the core due to the lack of biostratigraphic data. The identification of the Early Sheinwoodian Isotope Carbon Excursion (ESCIE) in the $\delta^{13}C$ data suggests that the base of the Tallbacken-1 core belongs predominantly in the lowermost Slite Group and that the bottom of the core is possibly close to the Hangvar Formation -Slite Group boundary. The deposition of these strata corresponds in time with the later parts of the Ireviken Event. Microfacies analysis reveals a carbonate platform that prograded into deeper waters and was terminated by a relative sea-level lowstand when minor karstification occurred.

Keywords: **S**ilurian, Gotland, Wenlock, carbon isotope stratigraphy, Slite Group, Hangvar Formation, sea level, carbonate platform.

Supervisor(s): Mikael Calner, Mikael Erlström

Subject: Bedrock Geology

Jan Radomski, Department of Geology, Lund University, Sölvegatan 12, SE-223 62 Lund, Sweden. E-mail: jan.radomski@outlook.com

Carbonate sedimentology and carbon isotope stratigraphy of the Tallbacken-1 core, early Wenlock Slite Group, Sweden

Jan Radomski

Radomski, J., 2018: Carbonate sedimentology and carbon isotope stratigraphy of the Tallbacken-1 core, early Wenlock Slite Group, Sweden. *Examensarbeten i geologi vid Lunds universitet*, Nr. 526, 28 sid. 45 hp.

Sammanfattning: Den mer än 700 m mäktiga lagerföljden på Gotland är erosionsresterna av vidsträckta karbonatplattformar som bildades i den Baltiska bassängen under silurperioden. Detta arbete fokuserar på stratigrafin och bergarterna i borrkärnan Tallbacken-1 som togs upp vid Stora Vede av Sveriges geologiska undersökning år 2006. Analys av kalkstenens mikrofacies tillsammans med analys av geofysiska data (gamma ray) från borrhålet ligger till grund för tolkning av depositionsmiljön och utvecklingen av karbonatplattformen under motsvarande tidsintervall. Fem identifierade mikrofaciesassociationer motsvarar fem olika depositionsmiljöer. Dessa representerar i stigande ordning genom kärnan: lågenergi yttre ramp, moderat energi mellersta ramp, högenergi revfront, hög energi revbälte och en lagunmiljö, dvs en uppgrundningssekvens till följd av revbältets progradering genom bassängen. Denna uppgrundning är avbruten av småskalig karstbildning. Utöver mikrofaciesanalys samlades 176 prover in från kärnan för $\delta^{13}C$-analys. Dessa data indikerar att basen av Tallbacken -1 kärnan stratigrafiskt ligger mycket nära gränsen mellan Hangvarformationen och Slitegruppen och att den senare delen av Ireviken Event (återhämtningsfasen) möjligen kan studeras i kärnans lägsta del.

Nyckelord: Silur, Gotland, wenlock, kolisotopstratigrafi, Slitegruppen, Hangvarformationen, havsnivå, karbonat-plattform.

Handledare: Mikael Calner, Mikael Erlström

Ämne: Berggrundsgeologi

Nyckelord: Silur, Gotland, wenlock, kolisotopstratigrafi, Slitegruppen, Hangvarformationen, havsnivå, karbonat-plattform.

Jan Radomski, Geologiska institutionen, Lunds universitet, Sölvegatan 12, 223 62 Lund, Sverige. E-post: jan.radomski@outlook.com

1 Introduction

In comparison with the abrupt climatic changes and mass extinction of the terminal Ordovician, the Silurian Period was for many years considered as being a stable and quiet time interval during the Phanerozoic Eon. Extensive epeiric seas stretched across the paleocontinents and carbonate platforms expanded in shallow seas where climate and environmental conditions were favorable (Bickert et al. 1997; Munnecke et al. 2010).

In contrast, a great number of sedimentological, paleontological and geochemical studies over the last 25 years have showed that the period was much more volatile than previously thought (Munnecke et al. 2003; Calner et al. 2004; summarized in Calner 2008). Research on the stable carbon and oxygen isotopes of Silurian rocks and fossils points toward a highly unstable ocean–atmosphere system (Samtleben et al. 1996; Saltzman, 2001; Kaljo et al. 2003). Positive carbon isotope excursions of early Wenlock, late Wenlock, late Ludlow ages and at the Silurian–Devonian boundary clearly reflect major changes in the ocean-atmosphere system in the relatively short Silurian period in comparison to other systems of the Phanerozoic Eon (Munnecke et al. 2010). The magnitude of those excursions is very high in contrast to those from the Mesozoic and Cenozoic, however the mechanisms responsible are not entirely clear (Munnecke et al. 2010).

A long series of studies (Jeppsson, 1990,1997; Aldridge et al. 1993; Jeppsson and Männik, 1993; Loydell, 1993,1994; Calner and Jeppsson, 2003; Calner, 2005; Calner 2008; Cramer et al. 2010b; Melchin et al. 2012; Jarochowska and Munnecke 2015; Trotter et al. 2016; among others) show that marine life was exposed to multiple biodiversity crises and extinctions in the Silurian. Those extinctions were closely related to sea level fluctuations and changes in the global carbon cycle (Calner 2008). The organisms that were impacted the most were graptolites, conodonts, chitinozoans, acritarchs, brachiopods, and reefs (Calner, 2008).

In chronological order, the three major extinctions during this period were the early Silurian Ireviken Event, the middle Silurian Mulde Event, and the late Silurian Lau Event. Those extinctions have been studied thoroughly in multiple locations around the globe although the Silurian rocks of Gotland has been a focal point of interest for many years (Jeppsson et al. 1995; Jeppsson and Calner 2002; Munnecke et al. 2003, 2010; Valentine et al. 2003; Brand et al. 2006; Cramer et al. 2006; Calner, 2005, 2008; Eriksson et al. 2009, among others). Support for extinctions are evident through many studies, but comparable studies on the following recovery periods are scarce.

The aim of this master project is twofold. The first goal is to construct a profile and document the variations in carbonate microfacies through the early Wenlock of the Tallbacken-1 core, which was drilled in northwestern Gotland in 2006. The microfacies analysis forms a basis for the reconstruction of the evolution of the local paleoenvironment along with interpretation of relative sea level variations. According to Johnson (1996) and Loydell (1998) it is possible to see small fluctuations in relative sea level by close examination of the lithology, occurrences of hiatuses, facies movements, and changes within the environment of deposition on stable platforms. Following this methodology, an approach has been taken to better understand the time frame represented by the core section being studied; one of the questions being addressed is whether the core section includes the Ireviken Event or not.

The second task is to establish a high-resolution $\delta^{13}C$ stratigraphy of Tallbacken-1 core in order to facilitate correlation of the corresponding succession with more remote sections. $\delta^{13}C$ stratigraphy has become increasingly important within the field of stratigraphy over the last 20 years, especially within the Silurian System

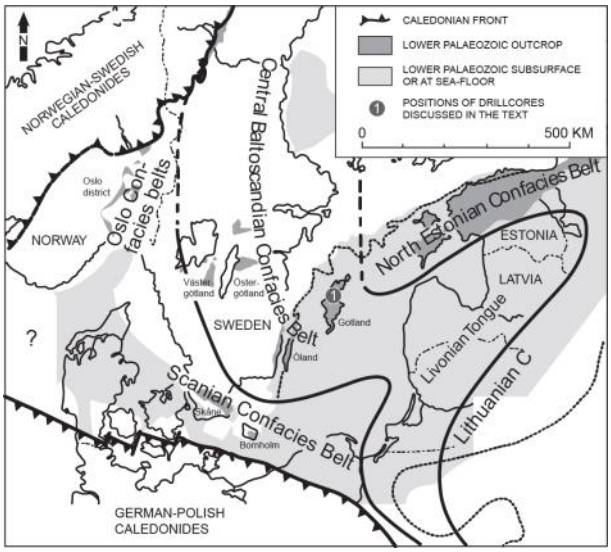

Fig. 1. Paleographic map of the Baltoscandian Basin showing the location of the studied Tallbacken core (1) (modified from Jaanusson 1995).

(Kaljo and Martma, 2006). Variations in the $\delta^{13}C$ excursions represent a disturbance within the global carbon cycle and climate itself (Cramer and Saltzman, 2005).

2 Geological setting and stratigraphy

In the early Silurian, the collision of Baltica and Laurentia took place starting the Scandian part of the Caledonian Orogeny (Baarli et al. 2003). At this time, the marine sediments, now forming Gotland, were deposited in the eastern parts of the Baltic basin. The basin was established on a Precambrian basement with a very low relief and had a moderate dip in southeastern direction (Baarli et al. 2003). During that time, the closing of the Tornquist Sea took place along with the thrusting of eastern Avalonia above the edge of Baltica (Mona Lisa Working Group, 1997). At that point, Gotland was located southeast of the Norwegian-Swedish Caledonides, in the south parts of Fennoscandian shield and northeast of German-Polish Caledonides. (Fig. 1).

All of the bedrock on Gotland is of Silurian age. It consists of reef and associated stratified limestone, marlstone and subordinate siltstone and sandstone (Hede, 1960). Strata is lying mostly horizontally with a dip angle of less than 1° (Fig. 2; Calner and Jeppsson 2003). Due to the south-eastern dip of strata, the exposed succession on Gotland is oldest in the northwestern part of the island and becomes progressively younger towards the southeastern part of the island.

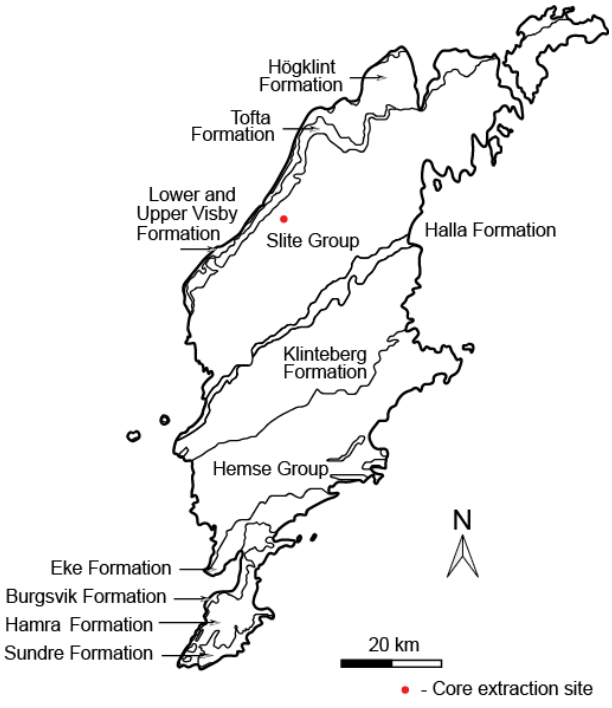

Fig. 2. Geological map of Gotland with the position of drill site (modified from Calner and Jeppsson 2004).

The succession on Gotland has been divided into thirteen topostratigraphic units by Hede (1960). He mapped the chief part of Gotland bedrock for the Swedish Geological Survey starting in 1921 (continued in 1929 and summarized in Hede 1960). The units recognized by him, starting from the oldest are: Lower Visby, Upper Visby, Högklint,, Tofta Beds, Slite Beds, (those above Slite not studied in this paper) Halla Beds, Mulde Beds, Klinteberg Beds, Hemse Beds, Eke Beds, Burgsvik Beds, Hamra Beds and Sundre Beds. Nowadays all the units mentioned above have a formation or group status (Fig. 3). In addition to the units defined by Hede, Calner (1999) defined and introduced the Fröjel Formation and Jeppsson (2008) defined and introduced the Hangvar Formation.

3 Materials and methods

The Tallbacken-1 core was retrieved at Stora Vede, ca 6.5 km southeast of Visby by the Swedish Geological Survey (SGU) in December 2006. The length of the core is 50.28 m and the diameter is 42 mm. The gamma ray data was collected shortly by SGU after drilling by Lund Technical university (Calner 2015 personal communication). The gamma ray log was used to help interpret sedimentary facies and help to understand the depositional environment. The lithology and faunal composition were investigated from nineteen thin sections (44.24m-3.66m) using a polarized light microscope. All the rock samples were cut in half, polished and studied using hand lens of 10x and 20x magnification along with a standard optical microscope. Dunham classification (1962) was used for classification of the various carbonate microfacies. Sampling for $\delta^{13}C_{carb}$ data was conducted in June 2014 using a hand-held micro-drill with 2 mm-sized bits. Sampling was done by aiming at micritic matrix and the avoidance of larger bioclasts or calcite veins.

A total of 176 samples were taken in approximately 0.3 m intervals throughout the entire core. All $\delta^{13}C$ samples were analyzed in the stable isotope lab of Michael Joachimski at GeoZentrum Nordbayern in Erlangen, Germany (Table 1).

Sample No.	$\delta^{13}C$ ‰	Depth (m)	Sample No.	$\delta^{13}C$ ‰	Depth (m)	Sample No.	$\delta^{13}C$ ‰	Depth (m)
Tal 1	2.19	50.13	Tal 65	-0.58	31.615	Tal 129	0.75	13.36
Tal 2	1.87	49.78	Tal 66	-0.24	31.335	Tal 130	0.56	13.1
Tal 3	1.50	49.43	Tal 67	-0.34	31.06	Tal 131	0.47	12.82
Tal 4	1.30	49.21	Tal 68	-0.29	30.815	Tal 132	0.51	12.535
Tal 5	1.77	50.13	Tal 69	-0.41	30.525	Tal 133	0.49	12.335
Tal 6	1.40	50.13	Tal 70	-0.20	30.325	Tal 134	0.51	12.055
Tal 7	1.31	50.13	Tal 71	0.06	30.045	Tal 135	0.58	11.8
Tal 8	1.11	48.12	Tal 72	0.14	29.745	Tal 136	0.61	11.525
Tal 9	0.58	47.73	Tal 73	0.09	29.43	Tal 137	0.63	11.265
Tal 10	1.05	47.465	Tal 74	-0.08	29.15	Tal 138	0.76	10.975
Tal 11	0.60	47.215	Tal 75	0.19	28.89	Tal 139	0.49	10.665
Tal 12	0.65	46.87	Tal 76	1.08	28.6	Tal 140	0.27	10.37
Tal 13	1.57	46.625	Tal 77	0.18	28.38	Tal 141	0.03	10.08
Tal 14	1.04	46.305	Tal 78	0.11	28.08	Tal 142	0.24	9.8
Tal 15	1.12	46.045	Tal 79	0.03	27.805	Tal 143	0.28	9.53
Tal 16	0.87	45.805	Tal 80	0.29	27.515	Tal 144	0.34	9.195
Tal 17	0.13	45.435	Tal 81	0.12	27.24	Tal 145	0.27	8.915
Tal 18	0.76	45.045	Tal 82	0.15	26.955	Tal 146	0.41	8.63
Tal 19	-0.28	44.815	Tal 83	0.21	26.705	Tal 147	0.44	8.43
Tal 20	-1.26	44.475	Tal 84	0.13	26.43	Tal 148	0.05	8.15
Tal 21	-0.68	41.175	Tal 85	0.19	26.115	Tal 149	0.03	7.84
Tal 22	-0.32	43.82	Tal 86	0.20	25.835	Tal 150	0.11	7.6
Tal 23	-0.36	43.47	Tal 87	0.25	25.54	Tal 151	0.44	7.305
Tal 24	0.23	43.115	Tal 88	0.27	25.265	Tal 152	0.33	7.03
Tal 25	0.06	42.83	Tal 89	0.25	24.965	Tal 153	0.21	6.725
Tal 26	-0.49	42.565	Tal 90	0.12	24.665	Tal 154	0.44	6.455
Tal 27	-0.61	42.29	Tal 91	0.20	24.365	Tal 155	0.39	6.155
Tal 28	-0.68	42	Tal 92	0.16	24.085	Tal 156	0.27	5.935
Tal 29	-0.66	41.695	Tal 93	0.07	23.81	Tal 157	0.24	5.665
Tal 30	-1.02	41.41	Tal 94	0.05	23.48	Tal 158	0.15	5.395
Tal 31	-0.93	41.155	Tal 95	0.24	23.18	Tal 159	0.34	5.165
Tal 32	-0.82	40.775	Tal 96	0.25	22.89	Tal 160	0.25	4.895
Tal 33	-0.39	40.585	Tal 97	0.24	22.69	Tal 161	0.24	4.665
Tal 34	-0.87	40.28	Tal 98	0.23	22.41	Tal 162	-0.04	3.92
Tal 35	-0.74	40	Tal 99	0.25	22.105	Tal 163	-0.43	3.62
Tal 36	-0.39	39.72	Tal 100	0.33	21.835	Tal 164	-0.67	3.32
Tal 37	-0.37	39.45	Tal 101	0.39	21.595	Tal 165	-0.48	3.025
Tal 38	-1.05	39.26	Tal 102	0.79	21.295	Tal 166	-0.19	2.74
Tal 39	-0.06	38.86	Tal 103	0.68	20.985	Tal 167	-0.36	2.43
Tal 40	-0.24	38.62	Tal 104	0.33	20.695	Tal 168	-0.30	2.135
Tal 41	-0.59	38.32	Tal 105	0.46	20.42	Tal 169	-0.43	1.855
Tal 42	-0.45	37.99	Tal 106	0.40	20.11	Tal 170	-0.33	1.585
Tal 43	-0.51	37.73	Tal 107	0.64	19.84	Tal 171	-0.27	1.315
Tal 44	-0.72	37.45	Tal 108	0.46	19.585	Tal 172	-0.19	1.035
Tal 45	-0.41	37.17	Tal 109	0.51	19.27	Tal 173	-0.33	0.855
Tal 46	-0.76	36.93	Tal 110	0.51	18.97	Tal 174	-0.44	0.54
Tal 47	0.43	36.665	Tal 111	0.48	18.635	Tal 175	-0.30	0.27
Tal 48	0.45	36.37	Tal 112	0.45	18.315	Tal 176	-0.59	0.01
Tal 49	-0.23	36.075	Tal 113	0.47	18.045			
Tal 50	-0.48	35.84	Tal 114	0.34	17.735			
Tal 51	0.07	35.54	Tal 115	0.47	17.445			
Tal 52	0.20	35.22	Tal 116	0.73	17.165			
Tal 53	-0.63	34.97	Tal 117	0.62	16.875			
Tal 54	-0.44	34.685	Tal 118	0.46	16.61			
Tal 55	-0.69	34.42	Tal 119	0.56	16.275			
Tal 56	-0.60	34.14	Tal 120	0.53	15.985			
Tal 57	-0.63	33.87	Tal 121	0.56	15.73			
Tal 58	-0.73	33.57	Tal 122	0.72	15.415			
Tal 59	-0.60	33.275	Tal 123	0.54	15.12			
Tal 60	-0.55	32.995	Tal 124	0.51	14.82			
Tal 61	-0.40	32.715	Tal 125	0.77	14.51			
Tal 62	-0.49	32.39	Tal 126	0.59	14.26			
Tal 63	-0.58	32.155	Tal 127	0.72	13.95			
Tal 64	0.02	31.915	Tal 128	0.32	13.655			

Table 1. 176 $\delta^{13}C$ samples and their analysis results from Tallbacken-1 core from Gotland, Sweden.

The samples were subsequently reacted with 100% phosphoric acid (density >1.9) at 75° C using a Kiel online preparation line connected to a ThermoFinnigan 252 masspectrometer. All $\delta^{13}C$ values are reported in permil relative to the V-PDB by assigning a $\delta^{13}C$ value of +1.95% to NBS19. Reproducibility for $\delta^{13}C$ analyses was monitored by replicate analysis of laboratory standards and was better than ±0.04 % (1s).

4 Latest Llandovery-Early Sheinwoodian stratigraphy of Gotland and the Early Sheinwoodian Carbon Isotope Excursion

The core was drilled in the western central part of the Slite Group outcrop belt. However, the exact stratigraphical level of the core site is unknown. It is expected that the core could reach below the Slite Group into underlying formations due to the knowledge of the local geology and the dip of the strata. The underlying units include the Lower Visby, Upper Visby, Högklint, Tofta and Hangvar formations that all are outcropping along the northwestern coast of Gotland, which is only a few kilometers from the drill site. These formations have received substantial scientific attention due to the presence of the Ireviken Event (Jeppsson, 1997, 2008; Bicker et al. 1997; Munnecke et al. 2003; Eriksson and Calner, 2005; Cramer, 2010b; among others) and the associated Early Sheinwoodian Carbon Isotope Excursion (ESCIE) (Fig. 3) within this stratigraphic interval (e.g. Lehnert et al. 2010). The isotope excursion is a globally important geochemical marker which is useful for correlation of strata. On Gotland it starts in the Upper Visby Formation and continues to near the base of the Slite Group (Bickert et al. 2007; Lehnert et al. 2010; Cramer et al. 2010a, b; Cramer et al. 2015).

One part of this thesis is to address the stratigraphic range of the Tallbacken-1 core by comparing the stable isotope stratigraphy recovered from the core with previously published carbon isotope data from outcrops in the area. Cramer et al. (2015, fig. 4) subdivided ESCIE in a series of sequences based on the morphology of the curve - including conodont biostratigraphy, sequence stratigraphy and $\delta^{13}C$ chemostratigraphy from Gotland, Sweden - into sequences IV – VIc, where sequence IV includes both Lower and Upper Visby Formations, sequence V covers Högklint Formation, sequence VIa includes Tofta Formation, sequence VIb corresponds to Hangvar Formation and sequence VIc begins at the Hangvar Formation-Slite Group boundary (Fig. 3). The falling limb of ESCIE starts in sequence VIa and continues into sequence VIc.

Below is a brief summary of the latest Llandovery through earliest Sheinwoodian stratigraphy of Gotland.

4.1 Lower Visby Formation

The Lower Visby Formation is the oldest Silurian stratigraphic unit on Gotland. The exposed thickness, according to Munnecke et al. (2003), is at least 12 meters, the base not being exposed above sea-level.

The Lower Visby Formation consists of bluish-grey, thin bedded and soft marlstone alternating with thin beds or lenses of greyish, argillaceous limestone (Laufeld, 1974). Thin *Halysites*-biostromes are present along with thin layers of brachiopod and bryozoan debris (Munnecke et al. 2003). Based on lithology and paleontology Munnecke et al. (2003) determined that this sequence was deposited in a distal shelf environment and below storm weather wave base. The boundary between the Lower and Upper Visby formations represents a sudden change in facies (Samtleben et al. 1996). Jeppsson (1989) noted a highly diverse conodont fauna within the Lower Visby Formation. Jeppsson (1989) reported a disappearance of a various species, above the last appearance datum of the rugose coral *Palaeocyclus porpita,* an index fossil for that formation.

A well-known ecostratigraphic marker horizon for the boundary between two Visby formations is the *Phaulactis* sp.rugose coral bed, which has a wide distribution on Gotland (Samtleben et al. 1996; Adomat *et al.* 2016). The *Phaulactis* layer can be traced ca 50 km along the north-west coast of the island and is 20 cm thick on average, but was observed to be over 1 meter thick in the south-west (Adomat et al. *2*016). The layer does not consist of only one single horizon of corals but various specimens of *P. angusta* that are occurring irregularly within the entire bed and form the *Phaulactis* layer (Adomat et al. *2*016).

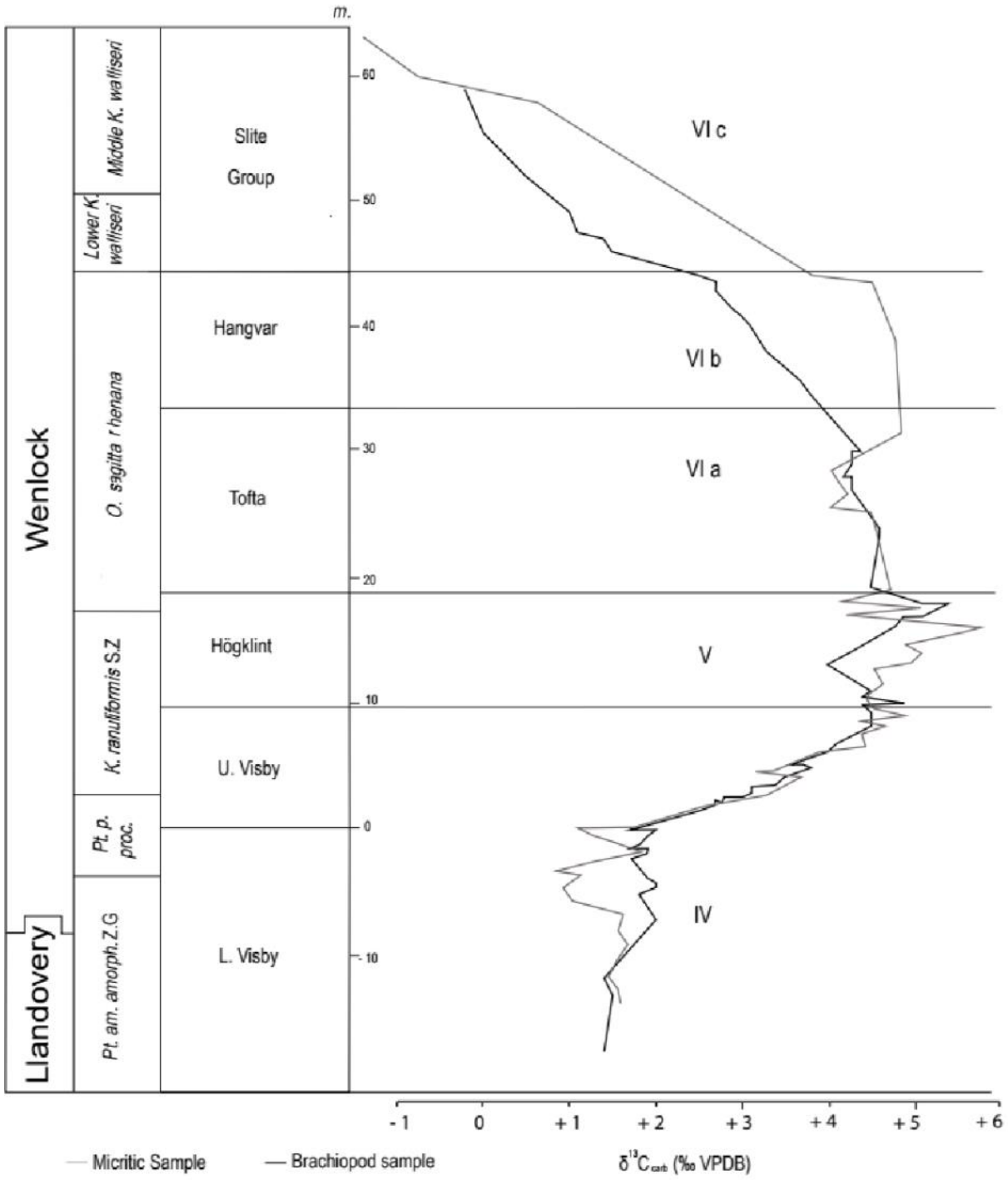

Fig. 3. Carbon isotope (δ^{13}Ccarb) data from Gotland, Sweden. The Early Sheinwodian Carbon Isotope Excursion (ESCIE) starts near the Llandovery-Wenlock boundary and the lower boundary of the Upper Visby Formation. The black line represents mean δ^{13}C values from brachiopod samples. The grey line represents δ^{13}C values from the micritic component (matrix) of limestone. VPDB – Vienna Pee Dee belemnite. Roman numerals (IV, V, VI) represent numbered sequence packages of the Silurian (modified from Cramer et al. 2010a, 2015).

4.2 Upper Visby Formation

The Upper Visby Formation is between the underlying Lower Visby Formation and the overlying Högklint Formation. It is composed of stratified bluish-grey soft marlstone and thin beds of greyish argillaceous limestone (Hede, 1960). The bedding is more irregular compared to the Lower Visby formation with an increased occurrence of wackestone and greenstone (Adomat et al. 2016).

The formation is 12 meters thick and in the upper part composed of mostly detrital limestone (Munnecke et al. 2003). Samtleben et al. (1996) noted that local tabulate rugose corals and stromatoporoids formed low elevated reef mounds. Jeppsson (1989) estimated that the conodont fauna was diminished to a maximum of six species.

The bioclastic limestone present in this formation formed a base for the reef mounds and was deposited in elevated water energy conditions Munnecke et al. (2003). The Upper Visby Formation was deposited at a lesser depth and more proximal than Lower Visby Formation, between storm wave base and fair- wave base average (Adomat et al. 2016).

4.3 Högklint Formation

The Upper Visby Formation is overlain by the Högklint Formation, which is composed of crinoidal limestone and prominent reef limestone that locally forms sea-stacks (Laufeld 1974; Watts 1981; Watts and Riding, 2000). Bioherms present in this formation were mainly built up by stromatoporides and reached ca 15 meters above the sea floor (Watts 1981). The largest patch reefs of the Högklint Formation are 100 to 150 meters wide and can be apart from one another with spacing anywhere from 150 to 350 meters (Watts and Riding, 2000). The reefs are situated in the upper part of a shallowing sequence and present a thumb-tack morphology, where agradational bioherms grew at the lower part of the reef and developed into progradational biostromes (Watts and Riding, 2000). Laufeld (1974) divided the Högklint Formation into four subunits (a-d). Unit "a" is 15 meters thick and dominated by biohermal and crinoidal limestone. Unit "b" is 14 -15 meters thick and composed of conglomeratic limestone and argillaceous limestone interposed with greyish-brown marlstone. Unit "c" is 4-5 meters thick according to Laufeld (1974) and consists of greyish to brownish grey limestone with stromatoporoids. Lastly, Unit "d" is only half a meter thick and known as Pterygotus or *Palaeophonus nuncius* beds. The latter unit is present only in the Visby area and characterized by black and reddish marlstone with reddish bituminous limestone (Laufeld, 1974).

The Pterygotus beds are characterized by well preserved fossils, in some cases even complete specimens of i.e. crinoid *Gissocrinus verrucosus* or starfish *Urasterella ruthveni leintwardinensis* (Franzen, 1979). An algal zone caps the Högklint Formation, forming a 0.3 - 0.6-meter-thick band that is traceable in the Visby area (Riding and Watts, 1991).

4.4 Tofta Formation

The Tofta Formation is overlying the Högklint Formation and is overlain by the Hangvar Formation. It is composed of oncolitic limestone and carbonate buildups of biostromal character, created predominantly by algae and stromatoporides (Samtleben et al. 1996). The formation is about 15 meters thick (Calner et al. 2004) and thins out towards the northeast (Laufeld, 1974) and also towards southwest (Hede, 1960). The formation consists of light grey to brownish grey limestone with abundant *Spongiostroma* (Laufeld, 1974). The upper boundary of the Tofta Formation is an unconformity that can reach down to Högklint in the northeastern and western parts of Gotland where Tofta deposits are sometimes missing (Samtleben et al. 1996). The Tofta Formation was deposited in a restricted, marginal marine environment (Hede, 1940).

4.5 Hangvar Formation

The Hangvar Formation is the most recent addition to the stratigraphy of Gotland and was introduced by Jeppsson (2008). It represents strata recognized in between the Tofta Formation and the Slite Group (Jeppsson 2008). Beds that were previously recognized as belonging to Högklint (Hede, 1940) were discovered to be younger than Tofta Formation and the same age as Slite "a" and "b" (Jeppsson, 2008). The Hangvar Formation is composed of what was once the upper part of the Tofta Formation and the former lowest part of Slite Group known as Slite "a" and "b", and are bounded below and above by unconformities (Jeppsson, 2008).

The Hangvar Formation, based on conodont zonation (*Ozarkodina sagitta rhenana* subzone 4 and 5), has been dated as middle Sheinwoodian. It represents the third sequence in the Wenlock of Gotland that ends with an erosional surface and reef generation (Jeppsson, 2008). Jeppsson (2008) describes two members within the Hangvar Formation (the lower and upper members). The lower one is argillaceous and accessible in distal areas. The upper one includes reef and associated deposits and is located SE and NE of Visby, as well as near eastern Fårö.

The biostratigraphic subdivision between the Hangvar Formation, Tofta Formation and the Slite Group is based on the absence of two similar conodont faunas. One is *Kockelella ranuliformis*, which is common in older faunas but not in Hangvar. The second one, *Kockelella walliseri* can be found more frequently in the younger faunas (Slite Group) (Jeppsson, 2008). Another reliable conodont marker is *Walliserodus*. It is found in collections from the lower Hangvar, but not present in the upper Hangvar unit and in marly areas where *Ozarkodina martinssoni* is rare, distinction between subzone 4 and 5 is only based on *Walliserodus* conodont range (Jeppsson 2008). For exact conodont collection locations see (Jeppsson, 2008, p. 36).

4.6 Slite Group

The Slite Group has a large outcrop area and is composed of two main lithofacies types. The first one is stratified limestone along with bioherms in the northern parts of the outcrop belt. The second one is marlstone interbedded with argillaceous limestone in the southwestern parts of the outcrop belt (Hede, 1960; Laufeld, 1974). Bedded limestones within Slite are composed of crinoidal and bryozoan debris and become more argillaceous towards South-Western direction (Laufeld and Bassett, 1981). The outcrops of the Slite Group are scattered across an area that is approximately 20 kilometers wide and 115 kilometers long (Fig.2; Jeppsson, 1983). Originally Hede (1960) subdivided the Slite Group into seven units a, b, c, d, e, f, g, which he referred to as members. In the revised stratigraphic scheme (Jeppsson 2008) “a” and “b” of the Slite Group form part of the Hangvar Formation. The first occurrence of the conodont *Kockelella walliseri* on Gotland is in the basal Slite Group (Jeppsson, 2008). Another conodont present in the basal Slite is *Hindeodella sagitta rhenana* (chiefly present in the Hangvar Formation) (Aldridge, 1975). The topmost part of the Slite Group is a thin unit rich in fine-grained siliciclastic, named Fröjel Formation by Calner (1999). The Fröjel Formation includes the Svarvare Mudstone and Gannarve Siltstone members. The thickness of Fröjel Formation is estimated to be between 9 and 11 meters (Calner, 1999). The total thickness of the Slite Group was calculated by Hede (1960) to be approximately 100 meters. According to Jeppsson (2008), the Slite Group is much thicker than thickness previously specified by Hede.

5 Core Description

5.1 Lithology, Gamma ray API and Carbon isotope stratigraphy

Lithological description, Gamma ray API and $\delta^{13}C$ data were used to study the Tallbacken-1 core. Carbonate microfacies were defined based on the sedimentary characteristics with respect to Dunham (1962) classification. Gamma ray measurements were evaluated to better understand the stratigraphic variation in lithology and sedimentary cyclicity. Microfacies recognition from the core may be reflected in the gamma ray signatures, which in return can lead to interpretation of sedimentary cycles with relation to changes in sediment supply and relative sea level (Krassay, 1998). The $\delta^{13}C$ data provides a reference for correlation with other sections.

Based on the observed stratigraphic variation in the carbonate microfacies, the core can be subdivided into five broad microfacies associations. These are named, in ascending order; A – Mudstone-Wackestone Association, B – Wackestone-Packstone Association, C – Floatstone-Rudstone Association, D – Boundstone Association, and E – Packstone-Grainstone Association.

5.1.1 (A) Mudstone-Wackestone Association

An interval with a strong dominance of the Mudstone-Wackestone microfacies between 50.28 m and 42.03 m is here referred to as the Mudstone-Wackestone Association. It consists of a limestone-marl alternation that is yellow and yellowish brown in color; sporadically grey and bluish grey. It is mainly composed of alternating mudstone and wackestone with occasional occurrence of packstone beds. It includes a small number of thin, sharp-based tempestite beds that

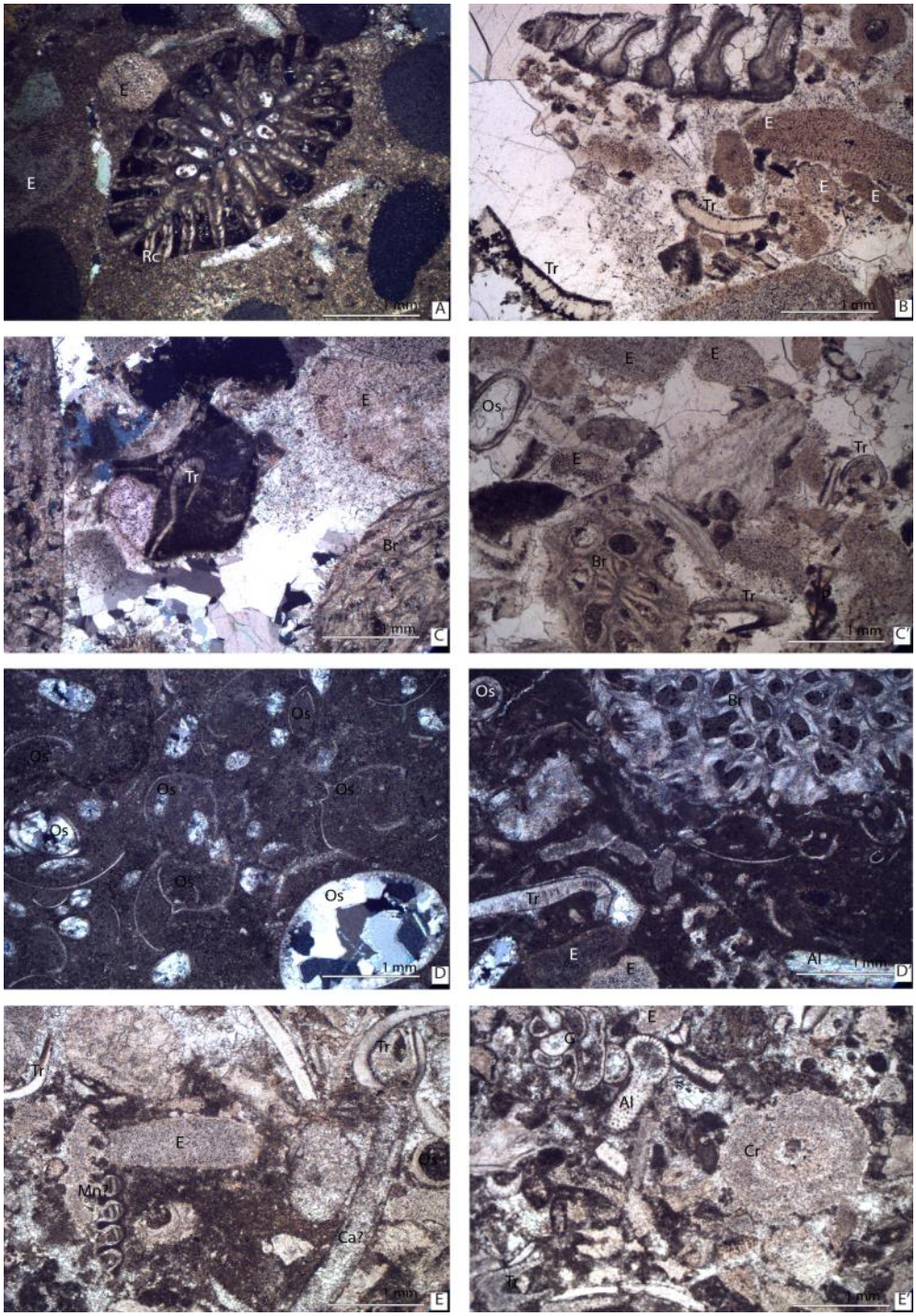

Fig. 4. Thin section composition representing marine invertebrates occurring throughout the studied core. Each letter (A-E) corresponds to the stratigraphic section that each thin plate belongs to. Key: Al – algae, Br – bryozoan, Ce – cephalopod fragment, Cr – crinoid, E – echinoderm fragment, G – gastropod, Mn – monograptus fragment, Os – ostracod, Rc- rugose coral Tr – trilobite. In thin section "A" notice most likely open-marine pelagic sediment with white patches of calcium carbonate cement surrounding the coral, some of which are recrystallized. "B" notice evidence of micrtization present on the trilobite pieces, their surface is uneven due to microborings. Looking at thin section "C" we observe perfectly preserved trilobite piece known as "Shepherd's crook" surrounded by micritic, dark organic material of uncertain affinity. Sparry calcite cement rims are growing on the dark material and the bryozoan piece present. "C" notice a plant lookalike (Charophyta?) fragment in the bottom right part of the thinsection. At the top left corner, we observe an ostracod filled with calcite cement along with other skeletal fragments surrounded by the same cement. Thin section "D" represents multiple thin wall ostracods with majority being single valve, settled in soft muddy sediment accompanied by a few thick wall cement filled ostracods. Notice spikes that would prevent them from sinking. Sample "D" is recognized as a bioclastic floatstone with bryozoan, ostracod, echinoderm, trilobite and calcifying algae pieces. Thin section "E" shows reworked pieces of trilobites, ostracods, mollusks and echinoderms. Notice what looks like monograptus towards the left side of the thinsection. Sample "E" represents another set of reworked fossils including algae, gastropod, crinoid and echinoderm pieces.

are either packstone or grainstone in composition. The tempestite beds as well as systematic packstone deposits vary from 3-10 cm in thickness. Within this section there is an abundance of microscopic trilobite cephalon fragments, occasional brachiopods and coral pieces (Fig.4 A) inside thin layers of storm deposits (Fig. 5 C-D).

The beginning of the gamma curve in the Mudstone-Wackestone Association (Fig.10) starts with the lowest value on curve being 33 API (American petroleum industry unit). The values show an increasing Gamma ray trend associated with the grains fining upward within this core section. The highest value reaches 79 API, but the rising trend continues onto the next facies association.

In the $\delta^{13}C$ record (Fig. 11.) a significant drop has been observed from the highest $\delta^{13}C$ value of +2.19‰ to a -1.26‰ within Mudstone-Wackestone Association of section A. This is the largest change measured in this carbonate excursion. There is no other $\delta^{13}C$ record of this magnitude from the early Wenlock period other than ESCIE that showed a rapid, negative isotope change. Therefore, it is most likely associated with the end of the Ireviken Event. After this initial drop, the curve slowly rises. There are a few fluctuations from positive to negative ‰ Vienna Pee Dee Belemnite standard (V-PDB). The curve rebounds to a value of +0.23 ‰ but is followed by another drop to -1.02 ‰.

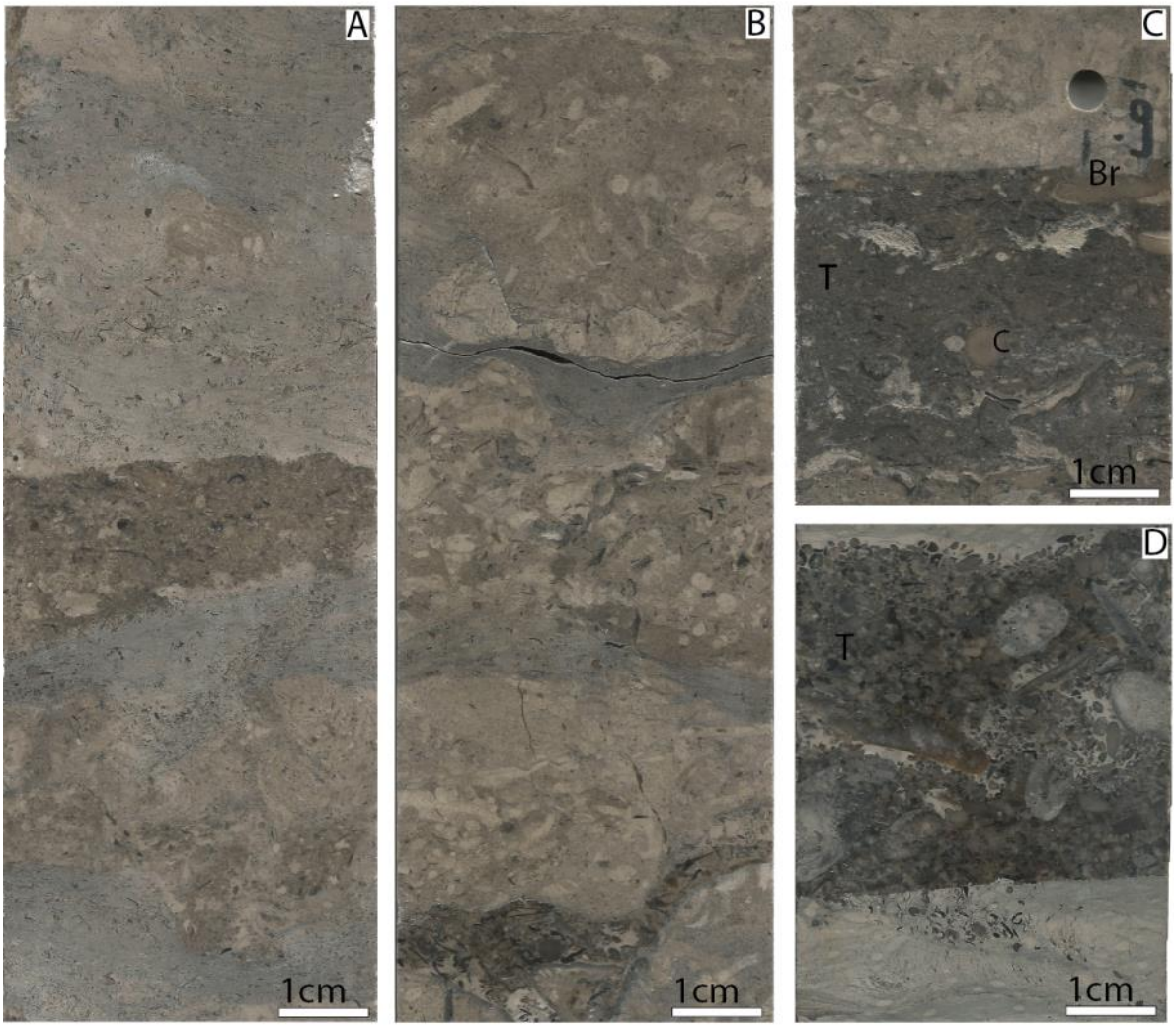

Fig. 5. Slabs from the Mudstone - Wackestone facies association (section A) of the studied core. A-D is the order of the decreasing depth from the bottom of the core, 49.9 m; 49.1 m; 47.9 m; 44.5 m. respectively. Br – bryozoan, C – coral, T- tempestite deposit. 9 – one of the zones used for C^{13} sampling. Slab "A" is a typical wackestone with mud supported matrix, containing multiple microscopic skeletal fragments. Notice a tempestite deposit in the middle with larger size skeletal fragments in comparison to the wackestone. Slab "B" represents a fragment of consecutive transition from laminated deposits to what looks like turbidites. Slab "C" represents a potential hardground with smooth upper surface along with encrusted bryozoan. Slab "D" represents tempestite deposits. Notice large clasts, skeletal fragments and sharp lower contact.

5.1.2 (B) Wackestone – Packstone Association

Between 42.03 m and 32.23 m, the core consists of limestone and marlstone that are grey to bluish and brownish grey, sporadically dark grey, in places yellow and yellowish brown to light brown. The first noteworthy packstone and grainstone beds are found here. Mudstone/ wackestone to packstone/grainstone beds are alternating in this facies association. A majority of argillaceous deposits are located at the bottom of this section and the amount of grain supported deposits increases towards the top. There are a few tempestite beds in the lowermost portion that are composed of packstone. The microfacies presented in Figure 6-C represent the thickest tempestite deposit (17 cm) and seems to have been produced by a significant storm episode or a few consecutive episodes due to bioturbated fragments of corals, bryozoans, cephalopod and vast amount of trilobite pieces present. Fossils are abundant in the bottom part of this section, some even visible with the naked eye (Fig. 6 A). There are abundant trilobite cephalon fragments present, accompanied by disarticulated brachiopod, bryozoan and coral fragments, although smaller in size in comparison with skeletal debris present within the tempestite beds.

In the bottom part of this facies association, the gamma ray values drop to 38 API but the general dirtying-up trend is pronounced. The highest value is reached at 104 API and is linked to the maximum flooding surface and maximum accommodation space at 39-meter core depth. From that point on, there is a steady decrease in the gamma values on the curve, associated with cleaning-up trend, showing that there is successively less argillaceous matrix in the rocks.

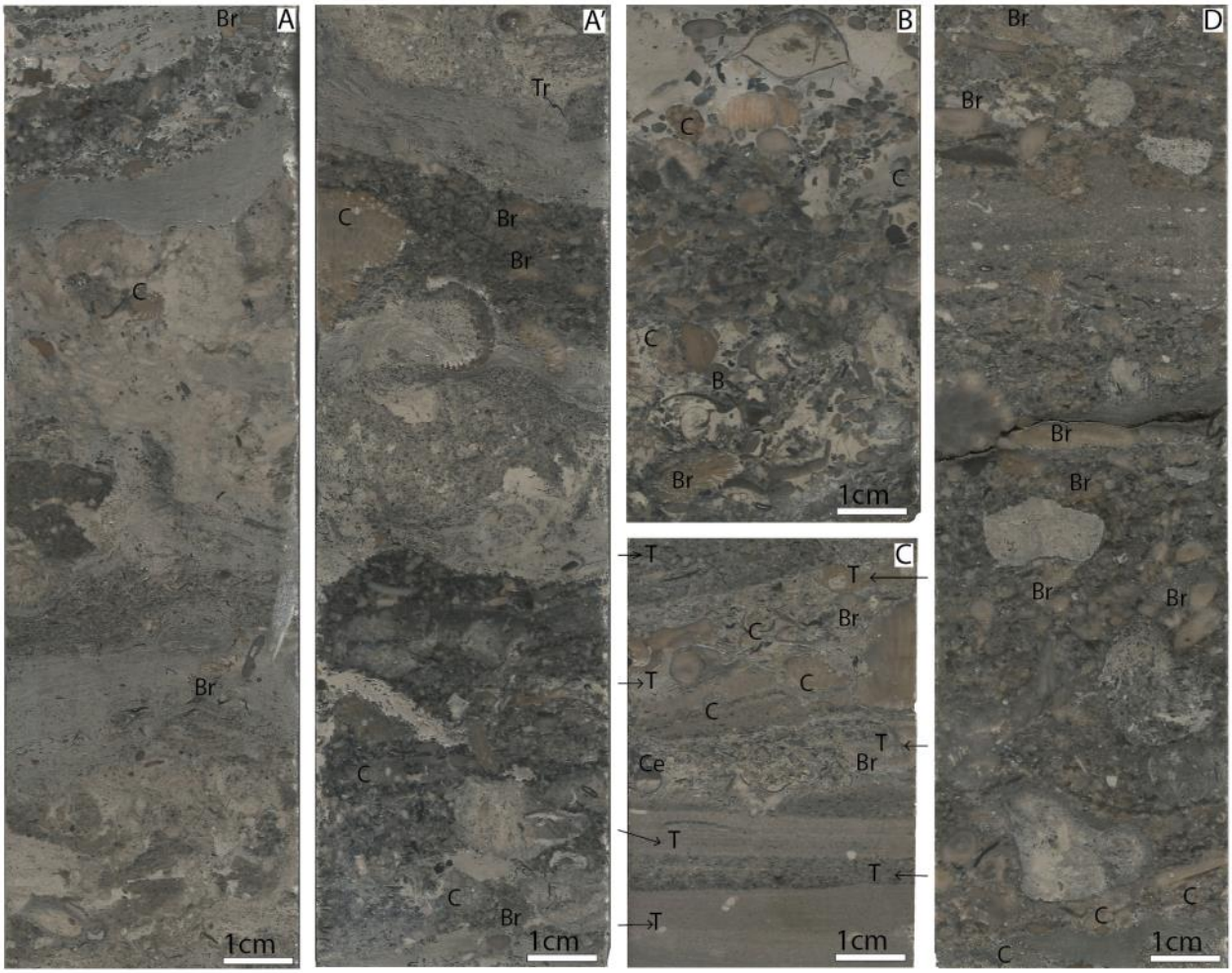

Fig. 6. Slabs from the Wackestone - Packstone facies association (section B) of the studied core. A-D is the order of the decreasing depth where A and A' are two parts of the same slab with depth of 42.1 m (A' 42m); 41.1m; 35.5 m; 34.1m. respectively. Br – bryozoan, C – coral, Ce – cephalopod, T- tempestite deposit. In slab C notice lamination at the bottom half of the examined piece followed by mixed skeletal fragments of corals and bryozoans as well as a cephalopod piece that stayed open during this event of rapid deposition. Looking at the quality of preservation of the fossil fragments within the above slabs it is obvious that

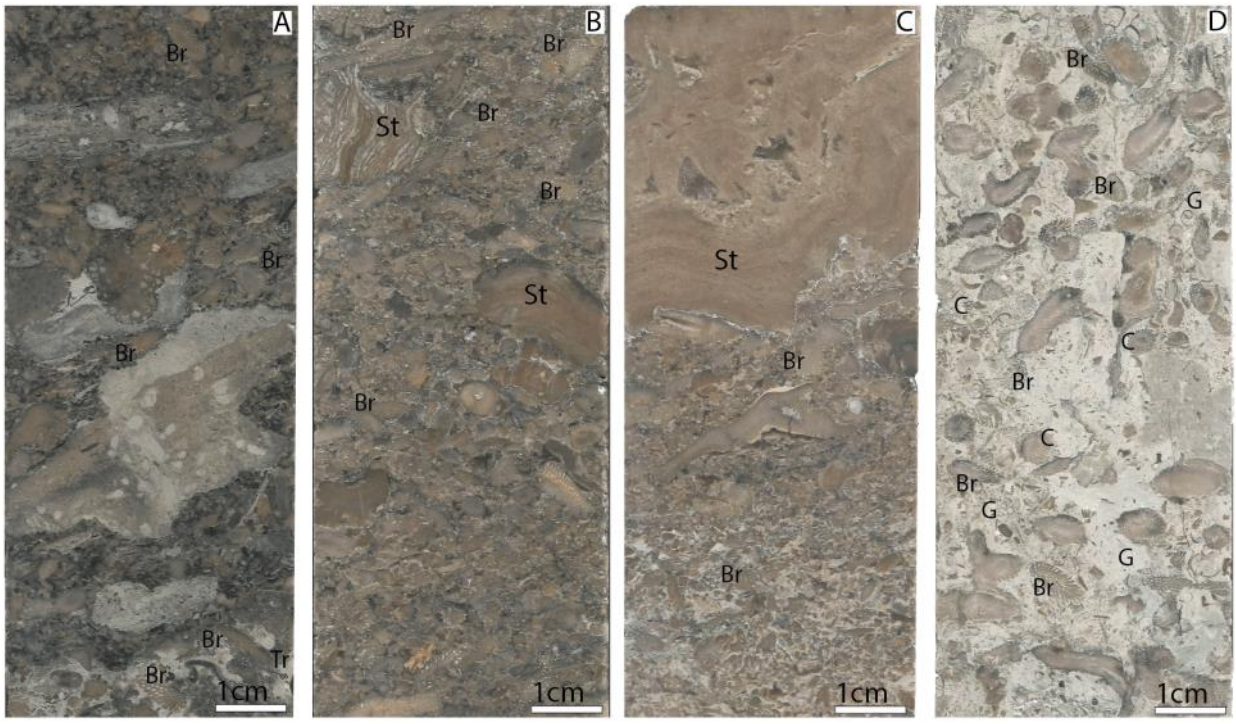

Fig. 7. Slabs from the Floatstone – Rudstone facies association (section C) of the studied core. A-D is the order of the decreasing depth: 31.9 m; 29 m; 25 m; 18.2 m. respectively. Br – bryozoan, C – coral, G – gastropod, St – stromatoporoid. Notice a significant increase in biological components with slab D being the most significant pure carbonate.

It reaches the lowest value of 26 API for this section at 32 and continues onto the next facies association.

At the beginning of the Wackestone - Packstone Association, values of $\delta^{13}C$ drop to -1.02 ‰. The excursion stays within negative $\delta^{13}C$ values until a minor rise to a value of +0.43‰ at 36.67 - meter core depth, and then becomes negative again at a value of -0.48‰ within the same one meter interval at 35.84 m. The excursion rises to 0.20‰ at 35.22 m and falls into negative values above 34.97 m until the end of this facies association at 32.23 m.

5.1.3 (C) Floatstone – Rudstone Association

The majority of the core section between 32.23 m and 16.26 m is represented by rudstone, with well abraded bioclasts, and subordinate floatstone, packstone and grainstone, mostly brown to light brown, greyish brown, grey and light grey in the beginning of this section. The upper part is predominantly light brown, brown and light greyish in places with its very top part being greyish white to greyish blue. Significant amounts of bryozoans are present throughout the entire section with an increasing trend towards the top part (Fig. 7 D). In the lower parts of this association are trilobite fragments. These are commonly known as "shepherd's crook" structures (Fig.4 C), along with some small shells, stromatoporoids, and coral pieces (Fig.7 A, B). The upper part of this section shows a variety of fossil fragments and intraclasts that are made of trilobite cephalon pieces, red crinoidal debris, along with small coral parts and abundant bryozoans (Fig.7 D).

The gamma ray values show a drop to 10 API at 30.65 m core depth, marking the end of the cleaning-up trend from the underlying Wackestone-Packstone facies association. The values increase rapidly to a 42 API after the drop. Aside from that instance, the gamma ray values stay at a low API value between 9 and 23 for the next 7 meters. This is associated with consistent rudstone microfacies within this part of the core. At 23.75 m the gamma values start to increase up to 44 API at 22.54 m and initiates a minor cleaning-up episode with the value dropping to 10 API at 19.27 m. At the end of this facies association, gamma value gradually reaches 33 API at 17.00 m which aligns with a microfacies transition.

The $\delta^{13}C$ ‰ curve continues to decrease in value, which is observed in the upper part of the Wackestone-Packstone facies association until a slow constant increase initiates at 30.53 m. The spike visible in the excursion at the beginning of this section is not considered due to the fact it was drilled in a marly part of the core. At ca 21.6 meters core depth, there is a high point in the excursion reaching from 0.39‰ to 0.79‰. Consequently, the $\delta^{13}C$ ‰ curve drops again, although

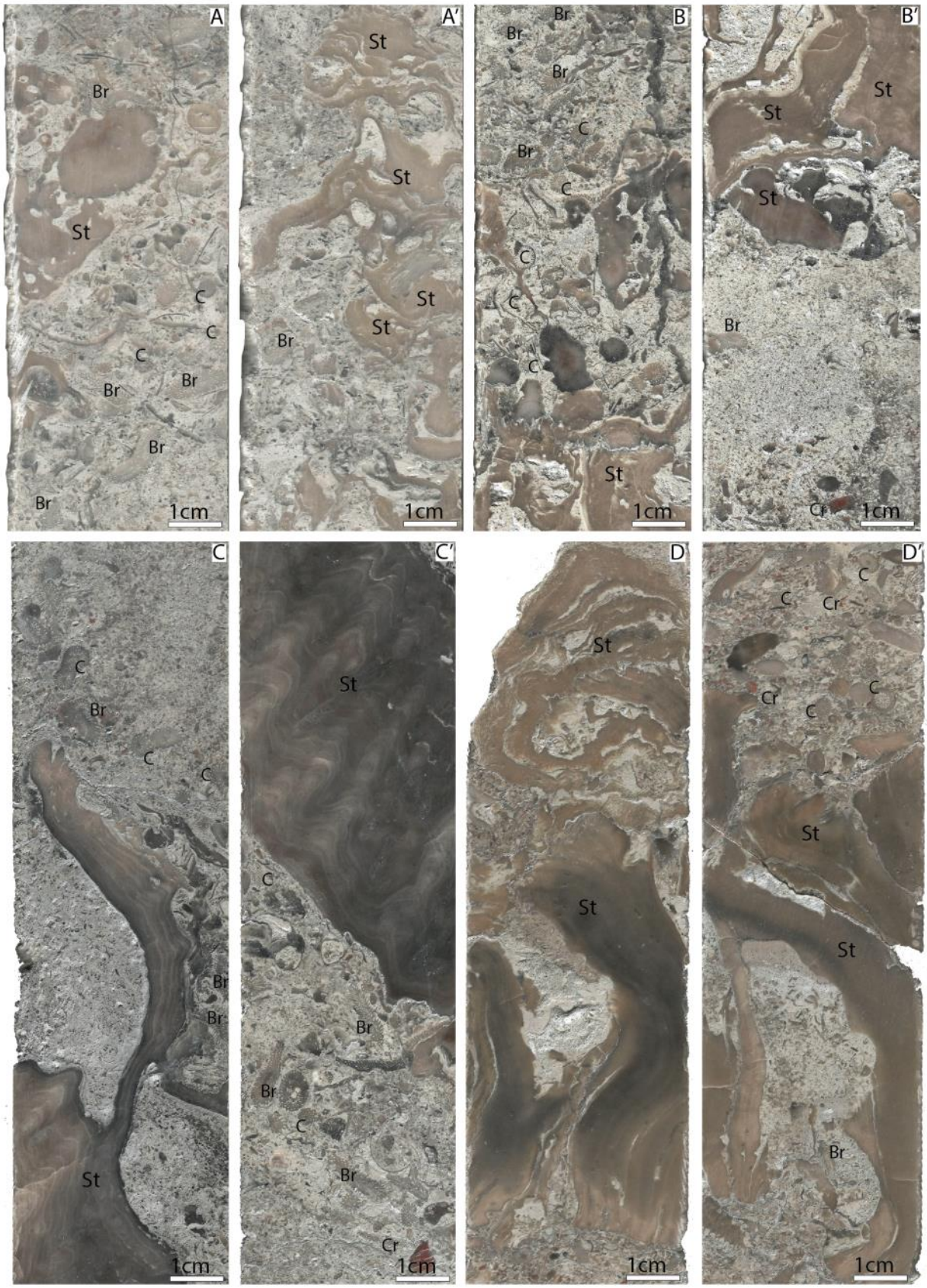

Fig. 8. Slabs from the Boundstone facies association (section D) of the studied core. A-D is the order of the decreasing depth where AandA' are two parts of the same slab from 15.1 m; 11.3m; 11 m; 5 m. respectively. Br – bryozoan, C – coral, Cr – crinoid, St – stromatoporoid. Notice black pebbles in slab B. Slabs C and D show well developed stromatoporoid structures. Slab C seems to have a cavity fill developed during subaerial exposure and followed by karstification. Slab D also shows cavity fills that give an impression of close to water surface conditions.

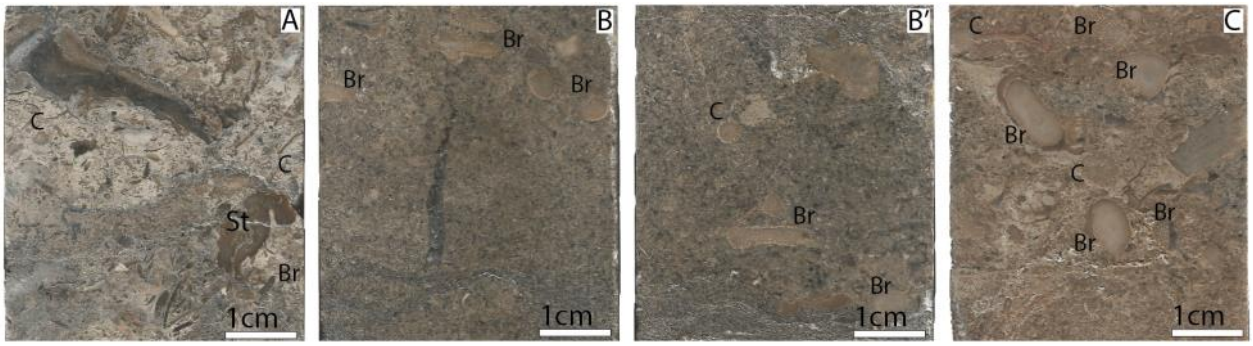

Fig. 9. Slabs from the Packstone-Grainstone facies association (section E) of the studied core. A-C is the order of the decreasing depth where BandB' are two parts of the same slab with depth of 4 m; 2.1 m; 0.4 m. respectively. Br – bryozoan, C – coral, St – stromatoporoid. Notice how biological components decrease from level presented in Slab A to just a few B and C. In slab C notice recrystallized bryozoans.

remains in a positive value without much fluctuation until it reaches the second-highest point. It is an increase from 0.34‰ at 17.74 m to 0.73‰ at 17.17 m in the upper part of Floatstone-Rudstone facies association.

5.1.4 (D) Boundstone Association

This part of the core is an 11.40 m long interval composed mostly of reef limestone, that is boundstone, between 16.26 m and 4.86 m. The lithology is light grey and bluish grey in the lower part with some grey, light brown and pinkish brown accents. The upper part of this core interval is grey and light grey to become mostly light brown, brown and light grey in places at its very top. This is where first *in situ* reef deposits occur (Fig. 8). This association can be subdivided in to two parts; one lower unit being 4.5-meter-thick with a thin subordinate layer (11 cm) of rudstone within. The upper unit is a little thinner, which is approximately 2.5 meters thick. Both boundstone units are divided by a 4.5-m-thick unit of alternating rudstone, floatstone, packstone, grainstone and a thin layer of mudstone. A disconformity is present between 11.32 m and 10.89 m within section D (Fig. 8 C, C'). Based on dissolution features and large sparry calcite fillings, the disconformity was formed by meteoric diagenesis and is a paleokarst surface. It has cut through stromatoporoid boundstone surrounded below and above by compacted debris of bryozoan and coral fragments along with occasional crinoids. Spaces between grain supported allochems are filled with white sparry calcite cement. This could be due to aragonite and high magnesium calcite being susceptible to dissolution with meteoric water into low magnesium calcite. It is also shown by a negative $\delta^{13}C$ shift in the data which could be caused by involvement of ^{13}C depleted water. The top of this section is composed of another stromatoporoid assemblage (Fig. 8 D, D').

At 16.77 m the gamma ray values decrease to ^{13} API at the lowermost portions of this facies association. The gamma values stay low but stable in this reef facies association and are interpreted as a second aggradation episode. The curve shows a minor decrease in values up to 6 API until 11 meters depth. At this point a rapid gamma spike has been observed, and is associated with a dirtying-upward occurrence and gamma value reaching 93 API at 8 meters depth. This is followed by a rapid decrease to 15 API and initiation of another rapid dirtying-up of lesser magnitude ending at 62 API with facies transition.

Within the boundstone association of section D, the $\delta^{13}C$ values are steadier and stay in a range between +0.32 ‰ and +0.76 until 10.98 m. At that point, a drop occurs from +0.76‰ to +0.03‰ which is associated with a disconformity with the inferred paleokarst. From there, the curve slowly builds up to a value of 0.43‰ followed by another decrease to 0.03‰ at 7.84 m. This is followed by another increase to 0.44‰ at 7.31 m and another drop to 0.21‰ at 6.73 m. The last minor increase of the values within the boundstone association brings it up to 0.34‰ at 5.17 m. This is a starting point for the last major descent in the carbon excursion and marks the endpoint for this section.

5.1.5 (E) Packstone – Grainstone Association

This 4.85-m-thick part represents the uppermost part of the core. It is composed of alternating grainstone, floatstone and rudstone; the last one is not present at all in the upper part of this interval. The colors are light yellowish brown to brown, or grey and light grey to brownish grey. Higher up in this core interval it becomes more darkish grey

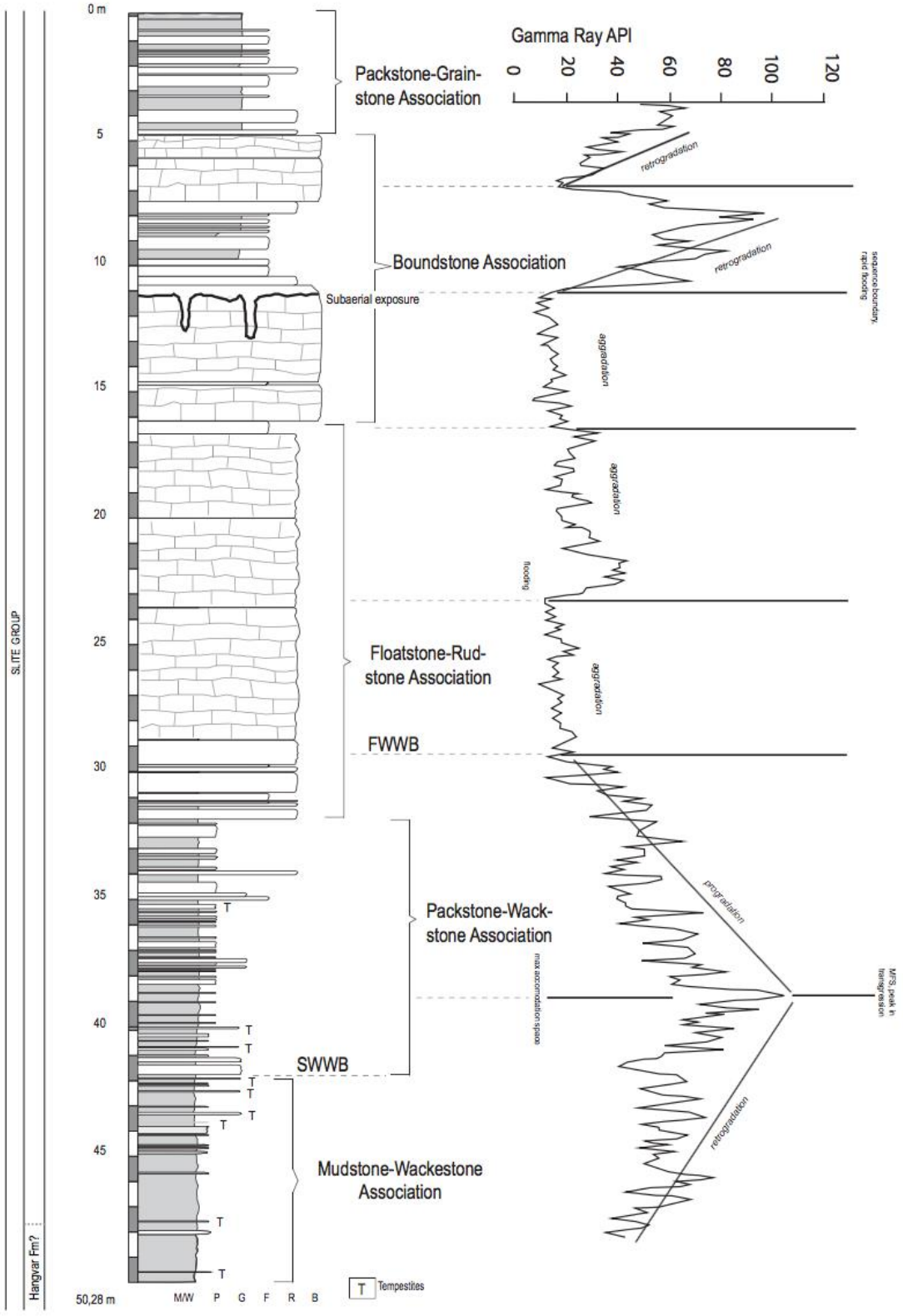

Fig. 10. Sedimentary profile showing the stratigraphic variation of carbonate microfacies in the Tallbacken-1 core along with gamma ray log data from the well. Matrix-rich microfacies such as mudstone and wackstone are associated with high gamma values whereas clean limestone such as grainstone, rudstone and boundstone are associated with low gamma values. Thus,the variation in the carbonate microfacies are mirrored by changing gamma values. Based on the combined data, five microfacies associations can be recognized. Note that frequent tempestite (storm) deposits are associated with depositional environments near –the storm weather wave base (SWWB) while being absent above the fair weather wave base (FWWB). The inferred boundary between the Hangvar Formation and the Slite Group is marked with a dotted line.

to greenish brown in places and pinkish brown to reddish brown at its very top. At its basal part, the abundance of fossils is still high (Fig.9 A). There are bryozoans, single gastropods and coral structures present, though it is noticeable that at the top part of this core section the fossil amount significantly decreases. Of the few uppermost pieces within core, one preserved a small amount of recrystallized and cemented bryozoan fragments.

Within this section the gamma ray curve ends since measuring started first at 3.96 meters below the ground surface. The values slowly increase to 68 API and shows a decrease that follows to the end of the curve and a value of 48 API. This interval is too short to describe any further details, although the trend clearly shows direction towards the low API values once again.

Another descent in the carbon excursion to -0.67 is visible between 5.17 m and 3.32 m. That is also where the packstone - grainstone association of section E begins. Even though there is a small rebound after the initial descent, the values for this interval stay negative until the very top of the studied core with last recorded value of -0.59 ‰ V-PDB.

6 Discussion

The various microfacies and microfacies associations described above represent depositional facies from different depositional depths within the carbonate platform. In order to interpret them in terms of bathymetry they need to be related to a carbonate platform model. The 'carbonate ramp' is a morphological variation of a carbonate platform and was first introduced by Ahr (1973). The term was later expanded and divided into homoclinal and distally steepened ramps, respectively, by Read (1980, 1982, 1985). The difference between the two types lies in their slope proximity and angle. Homoclinal ramp, as the name suggests, has a uniform dip of its slope towards the basin, whereas a distally steepened ramp features a steep, distal slope into deep water (Wright, 1986). A major part of the Slite Group was interpreted as representing a low angle or homoclinal ramp by Jacobsson (1997), due to the lack of redeposited sediments in deep water, slope break or any deep basin sediments present.

The homoclinal ramp model is used below in the interpretation of microfacies and their depositional environment. The model includes three distinct depositional environments. These are the outer ramp, below storm wave base, the middle ramp between storm wave base and the fair weather wave base, and the inner ramp, above the fair weather wave base.

6.1 Interpretation of microfacies associations

The paleoenvironment of Mudstone - Wackestone facies association (A) of the core, based on the abundance of matrix supported microfacies and microscopic skeletal fragments along with occasional thin graded beds (Fig. 5), is recognized as a low energy outer ramp of a carbonate platform. The thin graded beds have a sharp base and are interpreted as small scale turbidites. It is below the storm weather wave base and distal from the platform itself, which explains its main composition being mudstone and wackestone. Larger bioclasts are preserved within packstone tempestites, which the occurrence suggests episodic storm currents. In this precise scenario the outer ramp does not represent great water depth due to its existence within an epeiric sea.

Wackestone - Packstone facies association (B) is interpreted as a low to moderate energy middle ramp environment. An increased number of tempestites with larger fossil fragments and a decrease in the occurrence of mudstone and wackestone suggest conditions of an increased energy. The material has been deposited above the storm wave weather base, although probably quite near it and below fair-weather wave base. Within this section the sediments are bioturbated and burrowed trilobite fragments are present (Fig. 4 B). The tempestite beds are coarser-grained and graded as noticeable in Fig.6 C.

Floatstone - Rudstone facies association (C) represents a depositional environment of mixed energy, inner ramp reef slope. Its bottom part has a slight variation between grainstone and floatstone below fair-weather wave base, but it is mostly composed of fossiliferous rudstone that is above fair weather wave base. The fossils are well preserved in the upper part of the section and have not been transported far from their source, which indicates near in situ conditions (Fig. 7 D).

Boundstone facies association (D) is recognized as mixed energy inner ramp reef setting. Originally composed of mostly bindstone and rudstone, it was interrupted by the paleokarst disconformity that marks a shift in deposition. It correlates well with gamma spike corresponding to the beginning of a transgression stage (Fig.10) and a negative shift in $\delta^{13}C$ data (Fig. 11). Presence of packstone, grainstone and floatstone

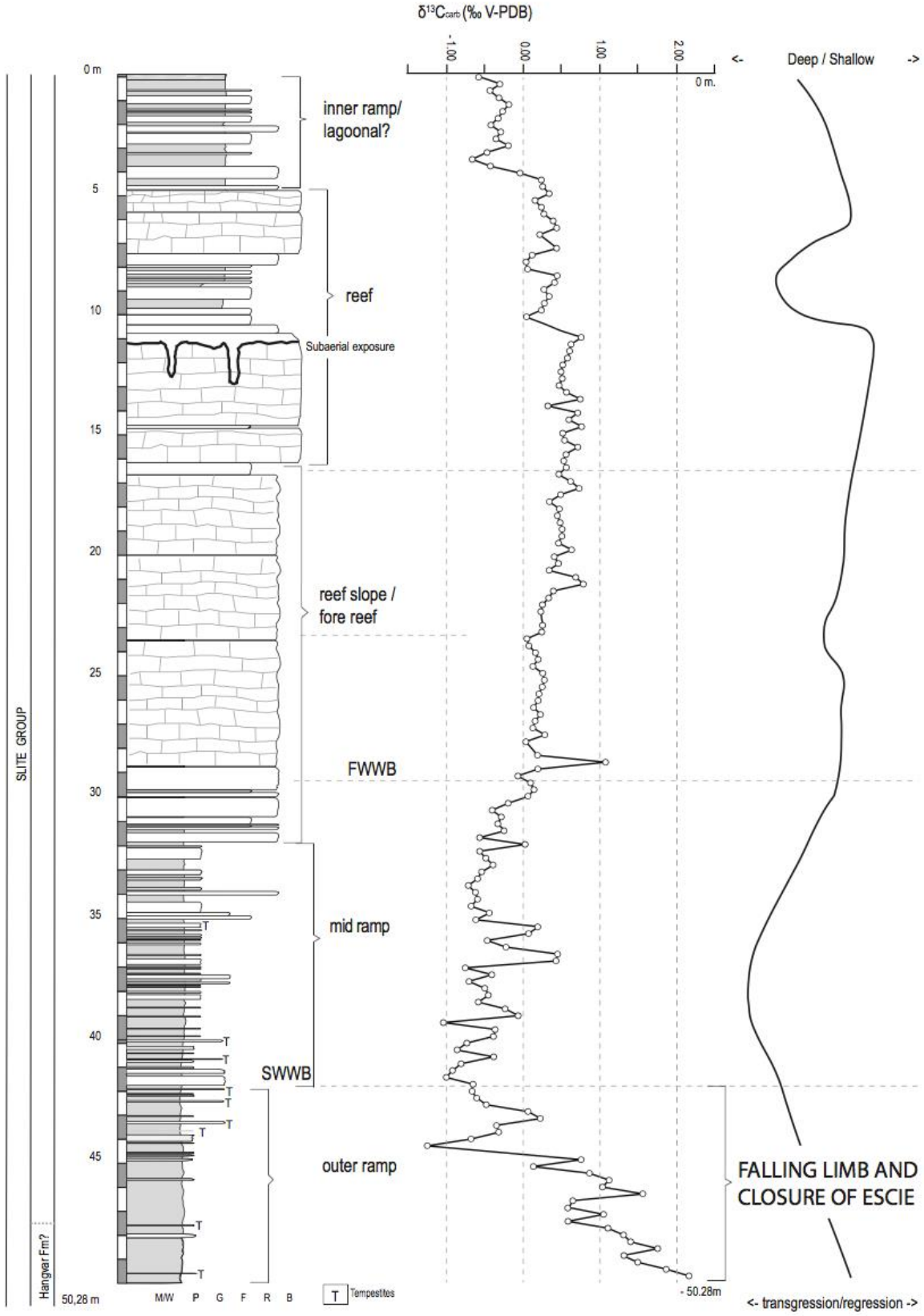

Fig. 11. Sedimentary profile of the studied Tallbacken-1 core along with the $\delta^{13}C$ isotope record and a general relative sea level curve. The steady decline of $\delta^{13}C$ values in the lowermost part of the core, from ca 2 permil to -1 permil, is interpreted as the falling limb of Early Sheinwoodian Carbonate Excursion (ESCIE). This means that the core section does not penetrate strata of the Ireviken Event, rather its early post-extinction strata and recovery phase. The sea level curve is based on observations of facies transitions, tempestite proximality analysis, bed thickness and fossil content, and reflects the progradation of a carbonate platform with reefs into the basin, that is, an overall relative regression.

above the erosional surface correlates to an increased water depth. The upper part of the section is again composed of rudstone and bindstone.

Packstone - Grainstone facies association (E) is interpreted as a low energy, inner ramp lagoonal facies. At the bottom of this part there are a couple of rudstone beds mixed with less fossiliferous grainstone. The fossils are scattered and seem to be washed into this section. Looking towards the top part, the rudstone are replaced by floatstone beds and the amount of organic material significantly decreases.

6.2 Sea-level history

The carbonate microfacies associations of the Tallbacken core (Fig.11) show a general shallowing upward, which reflects a relative regression and progradation of the carbonate platform.

In the lowermost part of the core, within the Mudstone-Wackestone microfacies association, the data shows the relative sea level rise linked with a period of transgression. Then, within Wackestone-Packstone microfacies, the fining upward trend reflecting transgression and retrogradation ends with Maximum Flooding Interval at 39 m depth. For the next 8 m of the core section, we've observed a cleaning upwards trend within the same microfacies. It is associated with progradation and sea level drop. For the next 19 m microfacies reflect a short aggradation episode and a slow paced regression associated with slow falling of sea level that ends at the transition between Boundstone Facies Association and Packstone-Grainstone Facies Association. At the 11 m deep, where Packstone-Grainstone Facies begin, there is sharp transgression episode associated with a shallowing followed by a rapid flooding until 8 m deep. At 6 m deep there is a transgression episode associated with a steady sea level rise.

A wide range of sea-level curves have been published for the Silurian period; e.g. Johnson (1996), Loydell (1998), Azmy et al. (1998), Johnson (2006), Haq and Schutter (2008), Spengler and Read (2010) among others; for a compilation see Munnecke et al. (2010, fig. 2). During the entire Silurian system, there were a total of ten sea-level high stands according to Johnson (2010), but according to the sea level curve by Haq and Shutter (2008) there were fifteen highstands during that time.

During the Sheinwoodian Stage, Johnson (2006, in Fig.1) showed sea level falling from an elevated level to a low-stand marked throughout the Ireviken Event. Analogically Loydell (1998) wrote about a sea level highstand followed by a drop, that was initiated in the *murchisoni* graptolite Biozone (early Sheinwoodian) and ended in the *ricartonensis* Zone (mid Sheinwoodian). A sea level rise occurred within the *ricartonensis* Zone that was reported by Loydell (1998) and Johnson (2006). According to Loydell, there was a sea level fall near the *ricartonensis* Zone upper boundary, but Johnson (2006) showed it already occurring in the *rigidus-pernei* graptolite Zone. Both authors agree there was a sea level fall during that time, with a minor zonation disagreement. A sea level rise that started after in the *rigidus-pernei* Zone, continued into the Homerian stage of Wenlock according to Johnson (2006, Fig.1). According to Munnecke et al. (2010) the sea level was rising in the early Silurian and dropped in late Silurian.

It's difficult to correlate these sea level fluctuations with the Tallbacken-1 core, however it does follow the pattern presented by Johnson (2006) during the Wenlock high stand. The sea level rise within the r*icartonensis* Zone can't be seen in the Tallbacken-1 core, although Johnson (2006) mentions a minor regression that follows. Consequently, this is analogical to the 39th meter depth where transgression ends and is followed by a regression. At 11 meters core depth we have observed karstification feature followed by rapid flooding that is associated with sea level rise and is acknowledged by Johnson (2006) in the *rigidus -pernei* Zone. This would agree with highstand continuing to the early Homerian according to Johnson (2006) just interrupted by transgression and regression occurring between 11th and 6th meter of the core. Calner and Säll (1999) described a sea level drop of minimum 16 m that took place during the Late Wenlock period associated with the uppermost C.*Lundgreni* graptolite Zone. This event most likely ended the early Homerian highstand trend.

As stated earlier, there has been a vast amount of Silurian sea level curves published in the past years (Munnecke et al. 2010) and they don't agree on the range of fluctuation during Silurian. For that reason, they can only be considered as general guidelines and not be used when working within smaller strata intervals. It would require further investigation to determine the exact scale that should be used for comparison of the Tallbacken 1 relative sea level with other locations.

6.3 Comparison of $\delta^{13}C$ data

The $\delta^{13}C$ carbon record of the Tallbacken-1 core is detailed in contrast to many other isotope data sets published from the Silurian of the Baltoscandian basin (e.g. Kaljo et al. 1997; Loydell, 1998; Kaljo and Martma, 2006). A similar basin environment that is described in this paper, based on the Tallbacken-1 core, was studied in the Priekule and Ohesaare drill cores from Estonia by Kaljo et al. (1997). The $\delta^{13}C$ values in the Tallbacken-1 core are not as high as those in the Estonian drill cores. It is beyond the scope of this study to answer the question of why it differs, but more importantly that there are some striking similarities present.

Both $\delta^{13}C$ records described by Kaljo et al. (1997) have different $\delta^{13}C$ values in comparison to those from Tallbacken-1, although the general trend is similar. At the beginning of the $\delta^{13}C$ record from Gotland, there is a significant decrease in $\delta^{13}C$ that occurs within the lower Mudstone-Wackestone Association of the core. The initial $\delta^{13}C$ drop visible in the lowermost sample in Tallbacken-1 is of smaller magnitude than in Estonia, but it can be related to negative changes in the early Sheinwoodian record from the Ohesaare and Priekule cores, which is +4.2‰ to -1.84‰ and +3.1‰ to -0.23‰, respectively (Kaljo et al. 1997). It is difficult to pinpoint further changes that are similar between the cores mentioned above, but what is clear, is the minimal variation visible in the $\delta^{13}C$ values in all three isotope curves in the aftermath of the Ireviken Event. Question arises if changes seen in the $\delta^{13}C$ record from the Tallbacken-1 core are of local phenomenon and did not occur widely throughout the Baltoscandian basin. The $\delta^{13}C$ record from Priekule shows that in deeper water the isotope curve is much smoother (Kaljo et al. 1997). This explains why values representing the period just after the ESCIE in the Priekule core (shelf depression), present a small amplitude between negative and positive changes within carbon record. $\delta^{13}C$ values from the same time interval in the Ohesaare core (shallow shelf) strengthen this hypothesis as they are slightly more elevated and vary more in comparison to those of the Priekule core record. Analogically the isotope values from Mudstone-Wackestone Association of the Tallbacken-1 core are lower due to their origination in deeper water (outer ramp).

According to Cramer et al. (2010a) and Lehnert et al. (2010), ESCIE on Gotland begins with` a shift to higher δ^{13} values within Lower *Pterospathodus procerus* conodont Zone. This is deducted from Cramer's logical reasoning on defining the start and end of the ESCIE. One should simply pick a point that marks the maximum positive rate of change and defines the increasing limb of the excursion at its onset (Cramer et al. 2010a). Analogically the end of the excursion would be where the isotope values drop below the previously defined starting point, which is in the basal Slite Group and in the Lower K. *walliseri* Zone on Gotland. Munnecke (et al. 2003) stated $\delta^{13}C$ values from Gotland to reach positive 4.5‰ V-PDB at the peak of the excursion. Cramer (2010a) stated that the $\delta^{13}C$ values averaged at a level of +1.5‰ before the ESCIE started on Gotland. In the Tallbacken-1 core the highest recorded $\delta^{13}C$ value is 2.19‰ in the lowermost section of the core. It then decreases steadily upwards through the lower 6 m of the core. This means that the very bottom of Tallbacken-1 core (50.28 – 44 m) would represent the falling limb of the ESCIE. According to Cramer et al. (2010b) the falling limb of ESCIE starts in the Tofta Formation and continues through the Hangvar Formation and into the basal Slite Group, which then is present in the lowermost meters of the Tallbacken-1 core. The boundary between sequences VIb and VIc of Cramer et al. (2015) is placed at the Hangvar Formation and Slite Group boundary and is associated with $\delta^{13}C$ values around 2permil (between the localities Hallagrund 1 and Hallarna 6). If $\delta^{13}C$ values are compared directly and numerically between outcrops (Calner 2017 – personal conversation) and the Tallbacken-1 core, the boundary between VIb and VIc is likely to be in the lowermost ca 2 m of the Tallbacken-1 core. Hence, the very initial drop of $\delta^{13}C$ values present in our data should reflect the end-part of the conclusion of this major $\delta^{13}C$ excursion on Gotland. It is very plausible, but not certain though without more detailed investigation, perhaps even an extension of the Tallbacken -1 core.

Based on the $\delta^{13}C$ data from Ohesaare core, the Tallbacken-1 core corresponds to the marly section of the upper Jaani and Jaagarahu stages of Wenlock age. $\delta^{13}C$ data from Priekule compared to Tallbacken-1 data links it to shale deposits within the Riga Formation.

While carbon isotope records are of great importance in understanding past climate and for stratigraphic correlation, further conclusions are

dependent on an understanding of the global carbon cycling (Saltzmann and Thomas, 2012). The understanding of this cycling is diminishing with increasing ageing of their records, and lack of reliable data on parameters such as ocean circulation, thus making our knowledge in this field very limited (Saltzmann and Thomas, 2012).

7 Conclusions

The Tallbacken-1 core was drilled and recovered from Stora Vede in north-western Gotland. The core section has been studied with respect to carbonate microfacies, carbon isotope stratigraphy, gamma ray well logging, and faunal composition.

The core includes a succession of carbonate microfacies that were deposited in a shallow intracratonic carbonate platform context. Five depositional environments were recognized: low energy outer ramp, moderate energy middle ramp, high energy reef slope, high energy reef belt and a relatively low energy lagoonal setting. Relative sea level has been assessed with the help of gamma ray log trends and carbonate microfacies. A moderate relative transgression ending with maximum flooding surface in the lower portions of the core suggests that the relative sea level was rising in the 50.28-38 m interval. From this level, the overall depositional environment shows progradation of a reef system across the middle and outer ramp environments, before the reef tract was exposed to meteoric diagenesis and minor paleokarst formation, implying short lived exposure of the reef to subaerial conditions. The second sea level rise was rapid and observed at 11 m core depth. It is associated with more argillaceous microfacies rich in terrigenous matter above the paleokarst surface.

The $\delta^{13}C$ data has been compared to similar records from the Priekule and Ohesaare drill cores studied by Kajlo et al. (1997). The three datasets show a similar trend related to a drastic fall in $\delta^{13}C$. The only documented event of this magnitude is associated with the Ireviken Event (the falling limb of ESCIE), which helps to constrain the stratigraphy of the Tallbacken-1 core. Combining gamma log data with $\delta^{13}C$ is of great significance in understanding the ancient carbonate deposits and their environment, it also allows us to correlate with other studies on a regional scale. Further investigation should be conducted for this data to be useful in global correlation.

8 Acknowledgements

I would like to express my sincere gratitude to my Supervisor Mikael Calner for giving me a chance to work on this project and all his time contributed on valuable comments, corrections and discussions without which this paper wouldn't be completed. Mikael Erlström as my second Supervisor along with SGU that provided the core and thin sections for this study. Professors and Staff that helped me within the Geology Department, either with their assistance or just a motivational conversation – Thank You, it made a difference to me and helped me to pursue my goal. Lastly, I want to thank my soulmate Agata, family and friends from Poland, Germany, Sweden and USA that never lost their faith in me and my determination to finish this thesis and supported me throughout the process.

9 References

Adomat, F., Munnecke, A., Kido. E., 2016. Mass occurrence of the large solitary rugose coral Phaulactis angusta at the boundary Lower/ Upper Visby Formation in the Silurian of Gotland, Sweden: paleoecology and depositional implications, GFF, 138:3, 393-409.

Ahr, W.M., 1973. The carbonate ramp - an alternative to the shelf model. Trans., Gulf Coast Assoc. Geol. Soc., 23: 221-225.

Aldridge, R.J. 1975a: The Silurian conodont Ozarkodina sagitta and its value in correlation. Paleontology 18, 323-332.

Aldridge, R. J., Jeppsson, L. and Dorning, K. J. 1993. Early Silurian oceanic episodes and events. Journal of the Geological Society, London, 150, 501–513.

Azmy, K., Veizer, J., Bassett, M.G., Copper, P., 1998. Oxygen and carbon isotopic composition of Silurian brachiopods: implications for coeval seawater and glaciations. GSA Bulletin 110, 1499–1512.

Baarli, B.G., Johnson, M.E., and Antoshkina, A.I., 2003: Silurian stratigraphy and paleogeography of Baltica. In E. Landing and M.E. Johnson (eds.): Silurian Lands and Seas, Paleogeography Outside of Laurentia. New York State Museum Bulletin 493, 3–34.

Bickert, T., Pätzold, J., Samtleben, C. and Munnecke, A. 1997. Paleoenvironmental changes in the Silurian indicated by stable isotopes in brachiopod shells from Gotland, Sweden. Geochimica et Cosmochimica Acta 61, 2717-2730.

Brand, U., Azmy, K., Veizer, J., (2006) Evaluation of the Salinic I tectonic, Cancañiariglacial and Ireviken biotic events: biochemostratigraphy of the Lower Silurian succession in the Niagara Gorge area, Canada and USA. Palaeogeography, Palaeoclimatology, Palaeoecology 241:192-213

Calner, M., 1999. Stratigraphy, facies development, and depositional dynamics of the Late Wenlock Fröjel Formation, Gotland, Sweden. GFF 121, 13-24.

Calner, M., 2005. Silurian carbonate platforms and extinction events – ecosystem changes exemplified from Gotland, Sweden. Facies, 51, Issue 1, 84–591.

Calner, M., 2008. Silurian global events – at the tipping point of climate change. In: Ashraf M.T. Elewa (ed.): Mass extinctions, pp. 21-58. Springer-Verlag. Berlin and Heidelberg

Calner, M., and Jeppsson, L., 2003. Carbonate platform evolution and conodont stratigraphy during the middle Silurian Mulde Event, Gotland, Sweden. Geological Magazine, 140, 173-203.

Calner, M., Jeppsson, L., and Munnecke, A. 2004. The Silurian of Gotland – Part I: Review of the stratigraphic framework, event stratigraphy, and stable carbon and oxygen isotope development. Erlanger geologische Abhandlungen, Sonderband 5, 113 - 131.

Calner, M., Säll, E., 1999. Transgressive oolites onlapping a Silurian rocky shoreline unconformity, Gotland, Sweden. GFF 121, 91–100.

Cramer, B. D., and Saltzman, M. R., 2005. Sequestration of 12C in deep ocean during the early Wenlock (Silurian) positive carbon isotope excursion. Palaeogeography, Palaeoclimatology, Palaeoecology, 219, 333-349.

Cramer, B.D., Kleffner, M.A., Saltzman, M.R., (2006) The Late Wenlock Mulde positive carbon isotope ($\delta^{13}C$) excursion in North America. GFF 128:85-90

Cramer, B.D., Loydell, D.K., Samtleben, C., Munnecke, A., Kaljo, D., Männik, P., Mart ma, T., Jeppsson, L., Kleffner, M.A., Barrick, J.E., Johnson, C.A., Emsbo, P., Joachimski, M.M., Saltzman, M.R., 2010a, Testing the limits of Paleozoic chronostratigraphic correlation via high Resolution (<500 kyr) integrated conodont, graptolite, and carbon isotope (d13C-carb) biochemostratigraphy across the Llandovery-Wenlock (Silurian) boundary: Is a unified Phanerozoic timescale achievable? Geological Society of America Bulletin, v. 122, 1710-1719.

Cramer, B.D., Kleffner, M.A., Brett, C.E., McLauglin, P.I., Jeppsson, L., Munnecke, A., and Samtleben, C., 2010b, Paleobiogeography, high-resolution stratigraphy and the future of Paleozoic biostratigraphy: Fine-scale diachroneity of the Wenlock (Silurian) conodont Kockelella walliseri: Palaeogeography, Palaeoclimatology, Palaeoecology, v.294, p. 232–241, doi:10.1016j.palaeo.2010.01.002.

Cramer, B.D., Vandenbroucke, T.R.A and. Ludvigson, G.A. 2015. High-Resolution Event Stratigraphy (HiRES) and the quantification of stratigraphic uncertainty: Silurian examples of the quest for precision in stratigraphy. Earth- Science Reviews, 141, 136-153.

Dunham, R.J., (1962) Classification of Carbonate Rocks According to Depositional Texture. In: Ham, W.E., Ed., Classification of Carbonate Rocks, AAPG, Tulsa, 108-121.

Eriksson, M.E., Calner, M., (Eds.), The Dynamic Silurian Earth. Sveriges Geologiska Undersökning, Rapporter och meddelanden, vol. 121 (2005), pp. 1-48

Eriksson, M.E., Nilsson, E.K., Jeppsson, L., 2009. Vertebrate extinctions and reorganizations dur ing the Late Silurian Lau Event. Geology 37, 739–742. doi:10.1130/g25709a.1

Franzén, C., 1979. Echinoderms. In: V. Jaanusson, S. Laufeld and R. Skoglund (eds), Lower Wenlock faunal and floral dynamics – Vattenfallet section, Gotland. Sveriges Geologiska Undersökning (C: Avhandlingar och uppsatser) 762, 216–224.

Haq, B.U., Schutter, S.R., 2008. A chronology of Paleozoic sea-level changes. Science 322, 64–68.

Hede, J.E., 1921, Gotlands Silurstratigrafi : Sveriges Geologiska Undersökning, C 305, 100 p.

Hede, J.E., 1929. Berggrunden (Silursystemet). In: Munthe, H., Hede, J.E. and Lundquist, G. Beskrivning till kartbladet Slite, 13-65. Sveriges Geologiska Undersökning Aa 169.

Hede, J.E., 1940, Berggrunden, in Lundqvist, G., Hede, J.E., and Sundius, N., eds., Beskrivning till kartbladet Visby and Lummelunda: Sveriges Geologiska Undersökning, Aa 183, 167 p.

Hede J.E., 1960. The Silurian of Gotland. In: Regnéll, G. and Hede, J.E. The Lower Paleozoic of Scania. The Silurian of Gotland. International Geological Congress XXI.

Jacobsson, M., 1997. Storm deposition on a Silurian prograding carbonate ramp, Slite Beds, Got land. GFF, 119, 199–206.

Jarachowska, E., Munnecke, A., 2015. Late Wenlock carbon isotope excursions and associated conodont fauna in the Podlasie Depression, eastern Poland: a not-so-big crisis? Geol. J. http:// dx.doi.org/10.1002/gj.2674 (online)

Jeppsson, L., 1983. Silurian conodont faunas from Gotland. Fossils and Strata, No. 15. pp. 121-144.

Jeppsson, L., 1989. Ett långt perspektiv — något om geologin vid Ireviken. Gotländskt Arkiv, 718.

Jeppsson, L., 1990. An oceanic model for lithological and faunal changes tested on the Silurian rec ord. Journal of the Geological Society, Lon don 147, 663-674.

Jeppsson, L., 1997. A new latest Telychian Sheinwoodian and Early Homerian (Early Silurian) Standard Conodont Zonation. Trans action of the Royal Society of Edinburgh Earth Sciences 88, 91-114.

Jeppsson, L., 2008. The Lower Wenlock Hangvar Formation - a sequence previously split be tween the Hogklint and Slite beds (Silurian, Gotland, Sweden). GFF, 130, 31-40.

Jeppsson, L., and Männik, P., 1993. High-resolution correlations between Gotland and Estonia near the base of the Wenlock. Terra Nova, 5, 348-358.

Jeppsson, L., Aldridge, R.J., Dorning, K.J., (1995) Wenlock (Silurian) oceanic episodes and events. J Geol Soc London 152, 487–498

Jeppsson, L., and Calner, M., 2003. The Silurian Mulde Event and a scenario for secundo-secundo events. Transaction of the Royal Society of Edinburgh Earth Sciences 93, 135-154.

Johnson, M.E., 1996. Stable cratonic sequences and a standard for Silurian Eustacy. In: Witzke, B.J., Ludvigson, G.A., Day, J.E.(Eds.), Paleozoic Sequence Stratigraphy: North American Perspectives—Views from the North American Craton. Special Publication-Geological Society of America, no. 306. GSA, Denver, pp. 203 – 211

Johnson, M.E., 2006. Relationship of Silurian sea-level fluctuations to oceanic episodes and events. GFF 128, 115–121.

Johnson, M.E., 2010. Tracking Silurian eustasy: Alignment of empirical evidence or pursuit of deductive reasoning? Palaeogeography, Palaeoclimatology, Palaeoecology 296, 276–284.

Lehnert, O., Männik, P. M., Joachimski, M., Michael, C., Frýda, J., 2010. Paleoclimate perturbations before the early Sheinwoodian Glaciation: A trigger for extinctions during the Ireviken Event. Palaeogeography, Palaeoclimatology, Palaeoecology 296, 320-331.

Johnson, M.E., 1996: Stable cratonic sequences and a standard for Silurian eustasy. In B.J. Witzke, G.A. Ludvigson, and J. Day (eds.): Paleozoic Sequence Stratigraphy: View from the North American Craton. Geological Society of America Special Paper 306, 203–211.

Kaljo, D., Kiipli, T., Martma, T., 1997. Carbon isotope event markers through the Wenlock–Pridoli sequence at Ohesaare (Estonia) and Priekule (Latvia). Palaeogeography, Palaeoclimatology, Palaeoecology 132, 211–223.

Kaljo, D., and Martma, T., and Mannik, P., and Viira, V., (2003). Implications of Gondwana glaciations in the Baltic late Ordovician and Silurian and a carbon isotopic

test of environmental cyclicity. Bulletin de la Societe Geologique de France. 174, 59-66.
Kaljo, D., and Martma, T., 2006. Application of car bon isotope stratigraphy to dating the Baltic Silurian rocks. GFF 128, 123-129.
Kaljo, D., Grytsenko, V., Martma, T., and Mõtus, M.-A., 2007, Three global carbon isotope shifts in the Silurian of Podolia (Ukraine): Stratigraphical implications: Estonian Journal of Earth Sciences, v. 56, p. 205–220.
Krassay, A., (1998) Outcrop and Drill Core Gamma -Ray Logging Integrated with Sequence Stratigraphy: Examples from Proterozoic Sedimentary Successions of Northern Australia. AGSO Journal of Australian Geology and Geophysics, 17, 285-300.
Laufeld, S., 1974. Silurian Chitinozoa from Gotland. Fossils and Strata 5, 1-130.
Laufeld, S., and Bassett, M.G. 1981. The anatomy of a Silurian carbonate platform. Episodes, 1981: 23-27
Loydell, D.K., (1998) 'Early Silurian sea-level changes', Geological Magazine, 135(4), pp. 447–471.
Loydell, DK., 1993. Upper Aeronian and lower Telychian (Llandovery) graptolites from western mid-Wales. Part 2. Monograph of the Palaeontographical Society 147, 55–180
Loydell, DK., 1994. Early Telychian changes in graptoloid diversity and sea level. Geological Journal 29, 355–368.
Loydell, D.K., 1998: Early Silurian sea-level changes. Geological Magazine 135, 447–471.
Melchin, M.J., Sadler, P.M., Cramer, B.D., 2012. The Silurian period. In: The Geologic Time Scale 2012, Gradstein, F.M., Ogg, J.G., Schmitz, M., Ogg, G. (eds.). Elsevier: Amsterdam; 525–558
Mona Lisa Working Group, 1997. Closure of the Tornquist Publ. 14. pp. 103–112. Sea: Con straints from MONA LISA deep seismic re flection data. Geology 25, 1071–1074.
Munnecke, A., Samtleben, C., Bickert, T., (2003) The Ireviken event in the lower Silurian of Gotland, Sweden-relation to similar Palaeozoic and Proterozoic events. Palaeogeogr Palaeoclimatol Palaeoecol 195, 99–124
Munnecke, A., Calner, M., Harper, Taylor, D.A., Servais, T., 2010. Ordovician and Silurian sea-water chemistry, sea level, and climate: a synopsis. Palaeogeography, Palaeocli- ma tology, Palaeoecology 296, 389–413.
Riding, R., and Watts, N., 1991: The lower Wenlock reef sequence of Gotland: facies and lithostratigraphy. Geologiska Föreningens i Stockholm Förhandlingar 113, 343–372.
Read, J. F., 1980, Carbonate ramp-to-basin transitions and foreland basin evolution, Middle Ordovician sequence, Virginia Appalachians: AAPG Bulletin, v. 64, p. 1575 -1612
Read, J.F., 1982. Carbonate platforms of passive (extensional) continental margins: types, characteristics and evolution. Tectonophysics, 81: 195-212.
Read, J.F., 1985. Carbonate platform facies models. Bull. Am. Assoc. Pet. Geol., 69: 1-21.
Saltzman, M.R., 2001. Silurian δ13C stratigraphy: A view from North America. Geology ; 29 (8): 671–674.
Saltzman, M.R., and Thomas, E., 2012, Carbon isotope stratigraphy, The Geologic Time Scale 2012, eds Gradstein, F., Ogg, J., Schmitz, M.D., and Ogg, G., p. 207-232.
Samtleben, C., Munnecke, A., Bickert, T., Patzold, J., 1996. The Silurian of Gotland (Sweden): Facies interpretation based on stable isotopes in brachiopod shells. Geologische Rundeschau 85, 278-292.
Spengler, A.E., Read, J.F., 2010. Sequence development on a sediment-starved, low accommodation epeiric carbonate ramp: Silurian Wabash Platform, USA midcontinent during icehouse to greenhouse transition. Sedimentary Geology 224, 84–115.
Valentine, J.L., Brock, G.A., Molloy, P.D., 2003. Linguliformean brachiopod faunal turnover across the Ireviken Event (Silurian) at Boree Creek, central-western New South Wales, Australia. Cour. Forsch.-Inst. Senckenberg, 242:301-327
Watts, N.R., 1981. Sedimentology and diagenesis of the Hogklint reefs and their associated sediments. Lower Silurian, Gotland, Sweden. Ph.D. Thesis: University College, Cardiff, 406 p.
Watts, N. R., and Riding, R., (2000), Growth of rigid high-relief patch reefs, Mid-Silurian, Gotland, Sweden. Sedimentology, 47: 979–994.
Wright, V.P., 1986. Facies sequences on a carbonate ramp: the Carboniferous Limestone of South Wales. Sedimentology, 33: 221-241.
Trotter, J. A., Williams, I. S., Barnes, C. R., Männik, P., and Simpson, A., 2016. New conodont d18O records of Silurian climate change: implications for environmental and biological events. Palaeogeogr. Palaeoclimatol. Palaeoecol. 443:34–48

Tidigare skrifter i serien ”Examensarbeten i Geologi vid Lunds universitet”:

472. Fouskopoulos Larsson, Anna, 2016: XRF -studie av sedimentära borrkärnor - en metodikstudie av programvarorna Q-spec och Tray-sum. (15 hp)
473. Jansson, Robin, 2016: Är ERT och Tidsdomän IP potentiella karteringsverktyg inom miljögeologi? (15 hp)
474. Heger, Katja, 2016: Makrofossilanalys av sediment från det tidig-holocena undervattenslandskapet vid Haväng, östra Skåne. (15 hp)
475. Swierz, Pia, 2016: Utvärdering av vattenkemisk data från Borgholm kommun och dess relation till geologiska förhållanden och markanvändning. (15 hp)
476. Mårdh, Joakim, 2016: WalkTEMundersökning vid Revingehed provpumpningsanläggning. (15 hp)
477. Rydberg, Elaine, 2016: Gummigranulat - En litteraturstudie över miljö- och hälsopåverkan vid användandet av gummigranulat. (15 hp)
478. Björnfors, Mark, 2016: Kusterosion och äldre kustdyners morfologi i Skälderviken. (15 hp)
479. Ringholm, Martin, 2016: Klimatutlöst matbrist i tidiga medeltida Europa, en jämförande studie mellan historiska dokument och paleoklimatarkiv. (15 hp)
480. Teilmann, Kim, 2016: Paleomagnetic dating of a mysterious lake record from the Kerguelen archipelago by matching to paleomagnetic field models. (15 hp)
481. Schönström, Jonas, 2016: Resistivitetsoch markradarmätning i Ängelholmsområdet - undersökning av korrosiva markstrukturer kring vattenledningar. (15 hp)
482. Martell, Josefin, 2016: A study of shockmetamorphic features in zircon from the Siljan impact structure, Sweden. (15 hp)
483. Rosvall, Markus, 2016: Spår av himlakroppskollisioner - bergarter i nedslagskratrar med fokus på Mien, Småland. (15 hp)
484. Olausson, My, 2016: Resistivitets- och IP - mätningar på den nedlagda deponin Gustavsfält i Halmstad. (30 hp)
485. Plan, Anders, 2016: Markradar- och resistivitetsmätningar – undersökningar utav korrosionsförhöjande markegenskaper kring fjärrvärmeledningar i Ängelholm. (15 hp)
486. Jennerheim, Jessica, 2016: Evaluation of methods to characterise the geochemistry of limestone and its fracturing in connection to heating. (45 hp)
487. Olsson, Pontus, 2016: Ekologiskt vatten från Lilla Klåveröd: en riskinventering för skydd av grundvatten. (15 hp)
488. Henriksson, Oskar, 2016: The Dynamics of Beryllium 10 transport and deposition in lake sediments. (15 hp)
489. Brådenmark, Niklas, 2016: Lower to Middle Ordovician carbonate sedimentology and stratigraphy of the Pakri peninsula, north-western Estonia. (45 hp)
490. Karlsson, Michelle, 2016: Utvärdering av metoderna DCIP och CSIA för identifiering av nedbrytningszoner för klorerade lösningsmedel: En studie av Färgaren 3 i Kristianstad. (45 hp)
491. Elali, Mohammed, 2016: Flygsanddyners inre uppbyggnad – georadarundersökning. (15 hp)
492. Preis-Bergdahl, Daniel, 2016: Evaluation of DC Resistivity and Time-Domain IP Tomography for Bedrock Characterisation at Önneslöv, Southern Sweden. (45 hp)
493. Kristensson, Johan, 2016: Formation evaluation of the Jurassic Stø and Nordmela formations in exploration well 7220/8-1, Barents Sea, Norway. (45 hp)
494. Larsson, Måns, 2016: TEM investigation on Challapampa aquifer, Oruro Bolivia. (45 hp)
495. Nylén, Fredrik, 2017: Utvärdering av borrhålskartering avseende kalksten för industriella ändamål, File Hajdarbrottet, Slite, Gotland. (45 hp)
496. Mårdh, Joakim, 2017: A geophysical survey (TEM; ERT) of the Punata alluvial fan, Bolivia. (45 hp)
497. Skoglund, Wiktor, 2017: Provenansstudie av detriala zirkoner från ett guldförande alluvium vid Ravlunda skjutfält, Skåne. (15 hp)
498. Bergcrantz, Jacob, 2017: Ett fönster till Kattegatts förflutna genom analys av bottenlevande foraminiferer. (15 hp)
499. O'Hare, Paschal, 2017: Multiradionuclide evidence for an extreme solar proton event around 2610 BP. (45 hp)
500. Goodship, Alastair, 2017: Dynamics of a retreating ice sheet: A LiDAR study in Värmland, SW Sweden. (45 hp)
501. Lindvall, Alma, 2017: Hur snabbt påverkas och nollställs luminiscenssignaler under naturliga ljusförhållanden? (15 hp)
502. Sköld, Carl, 2017: Analys av stabila isotoper med beräkning av blandningsförhållande i ett grundvattenmagasin i Älvkarleby-Skutskär. (15 hp)
503. Sällström, Oskar, 2017: Tolkning av geofysiska mätningar i hammarborrhål på södra Gotland. (15 hp)
504. Ahrenstedt, Viktor, 2017: Depositional history of the Neoproterozoic Visingsö Group, south-central Sweden. (15 hp)
505. Schou, Dagmar Juul, 2017: Geometry and faulting history of the Long Spur fault zone, Castle Hill

Basin, New Zealand. (15 hp)

506. Andersson, Setina, 2017: Skalbärande marina organismer och petrografi av tidigcampanska sediment i Kristianstadsbassängen – implikationer på paleomiljö. (15 hp)
507. Kempengren, Henrik, 2017: Föroreningsspridning från kustnära deponi: Applicering av Landsim 2.5 för modellering av lakvattentransport till Östersjön.(15 hp)
508. Ekborg, Charlotte, 2017: En studie på samband mellan jordmekaniska egenskaper och hydrodynamiska processer när erosion påverkar släntstabiliteten vid ökad nederbörd. (15 hp)
509. Silvén, Björn, 2017: LiDARstudie av glaciala landformer sydväst om Söderåsen, Skåne, Sverige. (15 hp)
510. Rönning, Lydia, 2017: Ceratopsida dinosauriers migrationsmönster under krittiden baserat på paleobiogeografi och fylogeni. (15 hp)
511. Engleson, Kristina, 2017: Miljökonsekvensbeskrivning Revinge brunnsfält. (15 hp)
512. Ingered, Mimmi, 2017: U-Pb datering av zirkon från migmatitisk gnejs i Delsjöområdet, Idefjordenterrängen. (15 hp)
513. Kervall, Hanna, 2017: EGS - framtidens geotermiska system. (15 hp)
514. Walheim, Karin, 2017: Kvartsmineralogins betydelse för en lyckad luminiscensdatering. (15 hp)
515. Aldenius, Erik, 2017: Lunds Geotermisystem, en utvärdering av 30 års drift.(15 hp)
516. Aulin, Linda, 2017: Constraining the duration of eruptions of the Rangitoto volcano, New Zealand, using paleomagnetism. (15 hp)
517. Hydén, Christina Engberg, 2017: Drumlinerna i Löberöd - Spår efter flera isrörelseriktningar i mellersta Skåne. (15 hp)
518. Svantesson, Fredrik, 2017: Metodik för kartläggning och klassificering av erosion och släntstabilitet i vattendrag. (45 hp)
519. Stjern, Rebecka, 2017: Hur påverkas luminiscenssignaler från kvarts under laboratorieförhållanden? (15 hp)
520. Karlstedt, Filippa, 2017: P-T estimation of the metamorphism of gabbro to garnet amphibolite at Herrestad, Eastern Segment of the Sveconorwegian orogen.(45 hp)
521. Önnervik, Oscar, 2017: Ooider som naturliga arkiv för förändringar i havens geokemi och jordens klimat. (15 hp)
522. Nilsson, Hanna, 2017: Kartläggning av sand och naturgrus med hjälp av resistivitetsmätning på Själland, Danmark.(15 hp)
523. Christensson, Lisa, 2017: Geofysisk undersökning av grundvattenskydd för planerad reservvattentäkt i Mjölkalånga, Hässleholms kommun. (15 hp)
524. Stamsnijder, Joaen, 2017: New geochronological constraints on the Klipriviersberg Group: defining a new Neoarchean large igneous province on the Kaapvaal Craton, South Africa. (45 hp)
525. 525. Becker Jensen, Amanda, 2017: Den eocena Furformationen i Danmark: exceptionella bevaringstillstånd har bidragit till att djurs mjukdelar fossiliserats.(15 hp)
526. 526. Radomski, Jan, 2018: Carbonate sedimentology and carbon isotope stratigraphy of the Tallbacken-1 core, early Wenlock Slite Group, Gotland, Sweden. (45 hp)

LUNDS UNIVERSITET

Geologiska institutionen
Lunds universitet
Sölvegatan 12, 223 62 Lund